ACS APPLIED MATERIALS & INTERFACES
Spotlight on Applications
www.acsami.org

Ligand Engineering of Polymer Nanocomposites: From the Simple to the Complex

Ying Li,[†] Timothy M. Krentz,[†] Lei Wang,[‡] Brian C. Benicewicz,[‡] and Linda S. Schadler*,[†]

[†]Department of Materials Science and Engineering, Rensselaer Polytechnic Institute, Troy, New York 12180, United States
[‡]Department of Chemistry and Biochemistry, University of South Carolina, Columbia, South Carolina 29208, United States

ABSTRACT: One key to optimizing the performance of polymer nanocomposites for high-tech applications is surface ligand engineering of the nanofiller, which has been used to either tune the nanofiller morphology or introduce additional functionalities. Ligand engineering can be relatively simple such as a single population of short molecules on the nanoparticle surface designed for matrix compatibility. It can also have complexity that includes bimodal (or multimodal) populations of ligands that enable relatively independent control of enthalpic and entropic interactions between the nanofiller and matrix as well as introduce additional functionality and dynamic control. In this Spotlight on Applications, we provide a brief review into the use of brush ligands to tune the thermodynamic interactions between nanofiller and matrix and then focus on the potential for surface ligand engineering to create exciting nanocomposites properties for optoelectronic and dielectric applications.

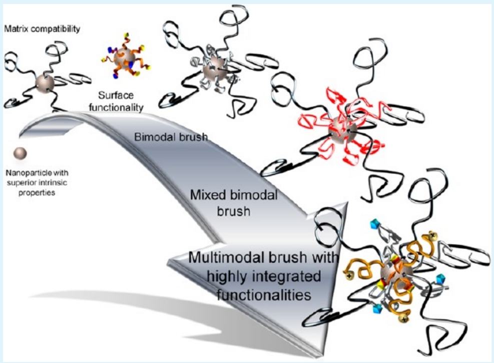

KEYWORDS: *surface ligand, surface functionalization, polymer brush, polymer nanocomposite, optoelectronic application, dielectric application, review*

INTRODUCTION

One of the critical knobs that can be turned to optimize the performance of polymer nanocomposites is surface ligand engineering of the nanofiller to control and enhance interface properties.[1−7] Surface ligand engineering can be as simple as the placement of short molecules on the nanofiller surface that improves the enthalpic compatibility between the filler and the matrix, or as complex as several populations of polymer chains that both add functionality and create controlled compatibility with the matrix, as illustrated in Figure 1. In the latter case, nanofiller assembly can be controlled independently from surface functionality. This paper summarizes focused work on surface ligand engineering and highlights applications that can benefit significantly from surface ligand engineering. We limit this article to spherical inorganic nanoparticles (nanofillers or nanoparticles for the sake of brevity). We stop short, however, of including isotropic inorganic nanoparticles carrying asymmetric functionalities, which is one class of Janus nanoparticles.[8,9] We briefly address the thermodynamic interactions controlling the nanofiller/matrix interactions as well as the chemical approaches to surface modification. We focus primarily on optoelectronic and dielectric applications in which the complexity of surface ligand engineering can potentially have the largest impact.

Predicting the interaction between surface-ligand-engineered nanofillers and small solvent molecules is relatively straightforward for spherical nanofillers. The dispersion is governed by a balance between the filler core/core enthalpic attraction, ideal translational entropy and, more importantly, the entropy-related steric hindrance provided by surface ligands.[10−13] When the fillers are sufficiently small, the enthalpic driving force for nanofiller agglomeration is primarily determined by the van der Waals (vdW) core/core interactions.[14]

When dispersing spherical nanofillers in a polymer or oligomeric matrix (even in solution), the enthalpic and entropic effects are more complex. Small surface molecules protect the nanofiller against aggregation either by sterically preventing clustering, or by minimizing enthalpic differences between the nanoparticles and the matrix, the latter of which is usually dominant.[15,16] Quantitatively, the enthalpic interactions can be described by "effective" or "cooperative" core/core vdW interaction energy between the grafted nanoparticles. One route to determining this enthalpic interaction uses the Hamaker constants of the pristine particle, the attached surface molecules, the matrix, and the dimension of the modified filler.[17−19] As the molecular weight of the surface molecule increases, the ligands are referred to as brushes. Monodisperse polymer brushes have been studied extensively since the early work of Alexander and de Gennes.[20−23] This seemingly simple approach to compatibilization, however, is complex. Intuition suggests that a high enough graft density and molecular weight

Special Issue: Applications of Hierarchical Polymer Materials from Nano to Macro

Received: November 24, 2013
Accepted: January 29, 2014
Published: January 29, 2014

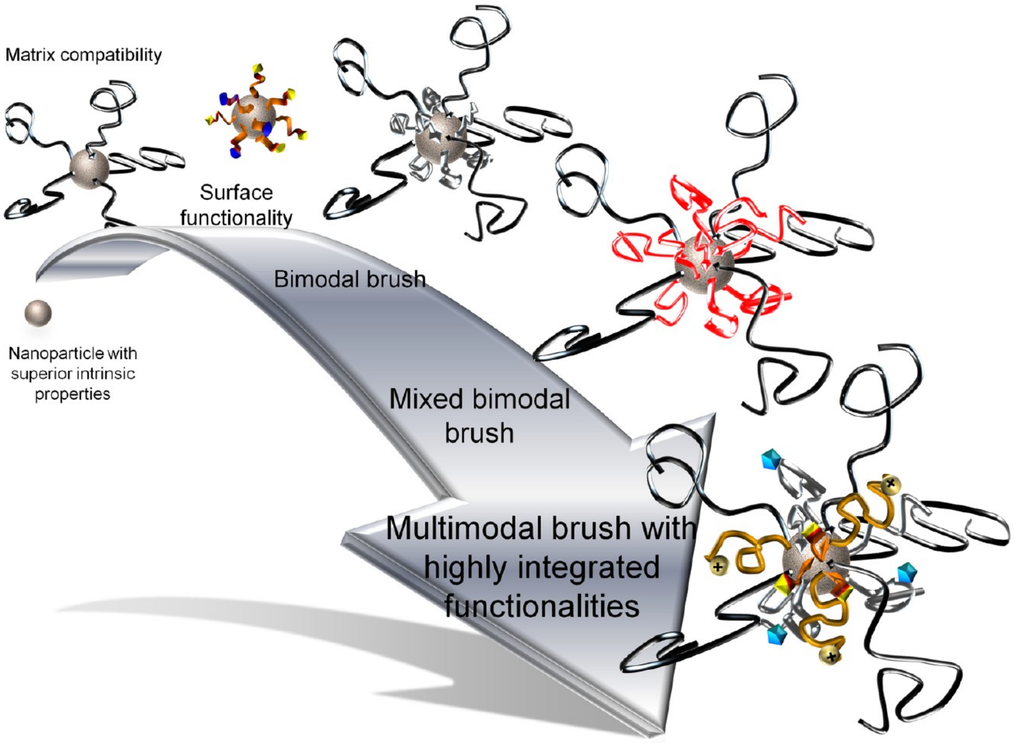

Figure 1. Surface ligand engineering going from the simplest to the most complex modifications (lab on a particle).

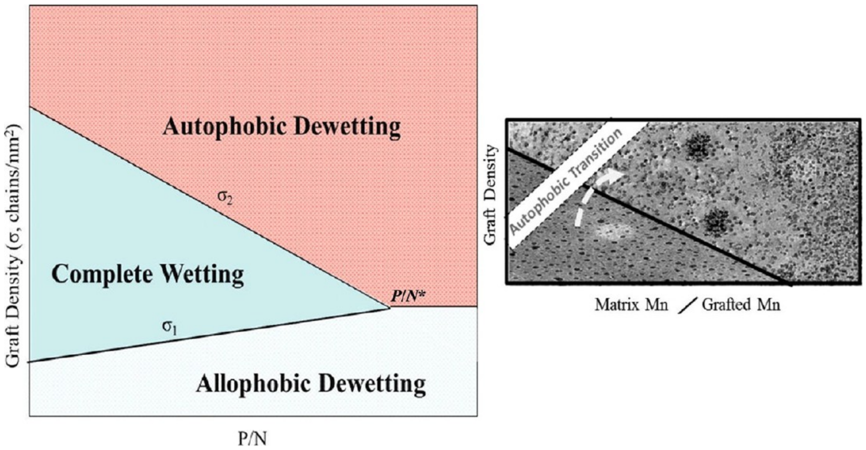

Figure 2. Schematic wetting (or compatibility) map as a function of the matrix and brush polymer molecular weights, P and N, and graft density, σ.[25] A window for achieving random dispersion exists between critical graft densities σ_1 and σ_2, and fillers are matrix-incompatible at all graft densities beyond a critical value of P/N. Adapted with permission from ref 25 (Copyright © 2012 American Chemical Society).

will screen the filler core/core vdW attractions and prevent allophobic dewetting. This intuition has been confirmed by the positive correlation between good dispersion and high surface coverage or a high value of $\sigma\sqrt{N}$ for short brushes, where σ is the brush graft density, and N is the degree of polymerization of the brush.[24] Entropy, however, plays an increasingly large role as the matrix molecular weight increases, and the entropic penalty for the matrix to penetrate the brush increases. Thus, at high graft density, autophobic dewetting (as evidenced by filler agglomeration) occurs.[25−29] As shown in Figure 2, the window between allophobic dewetting and autophobic dewetting becomes even narrower at higher matrix to brush molecular weight ratios (P/N).[25] For functional hybrid nanocomposites, which require a high molecular weight matrix with sufficient mechanical integrity and a low volume fraction of brush polymer to ensure high nanofiller loading (above ~10 vol %), the parameter space for desirable filler/matrix interaction is often limited.[18] The situation is even more challenging when functional groups or brushes that are incompatible with the matrix are incorporated into the surface ligand system.

As a means to overcome the entropic penalty that leads to autophobic dewetting and filler agglomeration, theoretical investigations have focused on understanding the influence of brush polydispersity on polymer brush behavior.[30−33] Such exploration is practical because polydispersity in molecular weight is common especially for industrial and commercial grade samples. It has been found that polydisperse polymer brushes facilitate the penetration, or wetting, of the brush layer by the matrix chains, and in turn stabilize the dispersion of grafted nanofillers even at high graft densities, where a

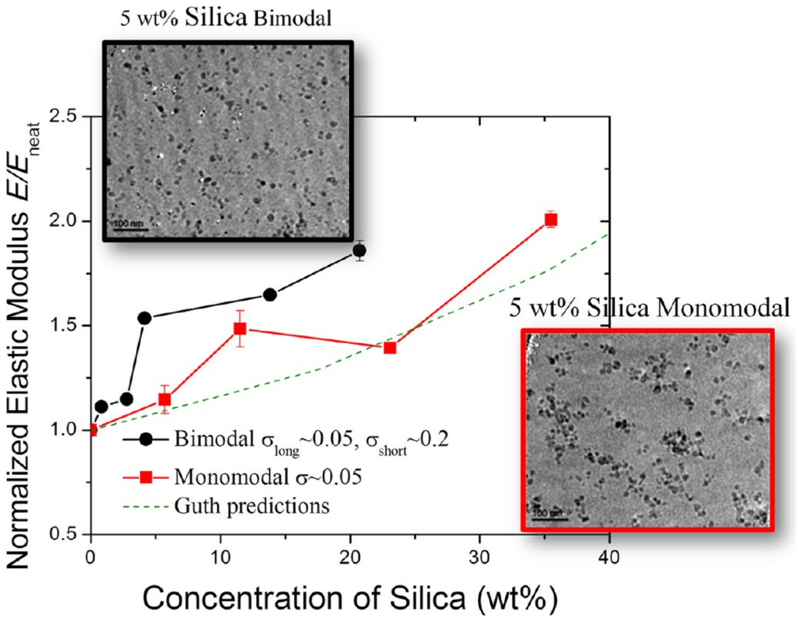

Figure 3. Comparison of the normalized indentation elastic modulus between bimodal brush systems (black line, ∼118 kg/mol long brush at ∼0.05 ch/nm^2 graft density and ∼7 kg/mol short brush at ∼0.2 ch/nm^2), monomodal brush systems (red line, graft densities and molecular weights almost identical to those of the long brushes of the bimodal systems), and Guth predictions for SiO_2 in the 96 kg/mol polystyrene matrix (green dash line). Inset: TEM images showing the dispersion of the corresponding bimodal (black border) and monomodal (red border) systems, scale bar 100 nm.[17,36] Reproduced with permission from ref 17 (copyright 2013 American Chemical Society) and ref 36 (copyright 2012 American Chemical Society).

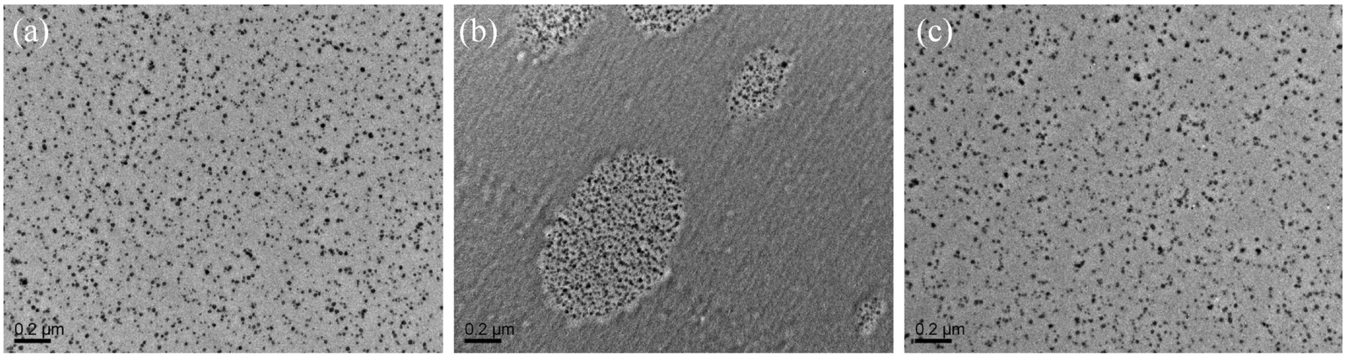

Figure 4. TEM micrographs of 5 wt % mixed-bimodal-brush-grafted SiO_2 nanoparticles, grafted with ∼205 kg/mol PMMA long brush at ∼0.67 ch/nm^2 graft density, and ∼2 kg/mol PS short brush at ∼0.26 ch/nm^2, dispersed in (a) ∼100 kg/mol PMMA, (b) ∼100 kg/mol PS, and (c) ∼300 kg/mol PMMA matrices, scale bar 0.2 μm.

monodisperse brush would cause aggregation.[32,33] The polydispersity of the matrix is also important and in systems where polydispersity is more commercially relevant, the window of brush molecular weight and graft density that leads to good dispersion increases.

As the simplest form of polydispersity, a polymer brush with bidisperse molecular weight is termed a bimodal brush. Bimodal brushes increase the controllable parameter space from brush length, graft density, and brush to matrix molecular weight ratio, to include long to short brush population ratio and effective graft density.[17,18,34−36] The power of this approach is that it provides a method for independently controlling the enthalpic and entropic interactions. The densely grafted short brushes enthalpically screen the vdW core/core attraction, which is especially critical for nanofiller/matrix systems with large surface energy mismatch. The sparsely grafted long brushes suppress entropic dewetting of high-molecular-weight polymer matrices. Early theoretical work on bimodal polymer brushes focused on their equilibrium conformation in a good solvent.[37−39] These studies have suggested independent density profiles of the long and short brush populations; and, the effect of bimodal distribution on brush conformation to be more significant for longer chains than shorter ones.[31,33] Such bidispersity has also been used to reduce the entropic surface tension of polymer brushes and suppress dewetting of thin polymer films.[40,41] In bulk nanocomposites, bidispersity decreases the driving force for agglomeration. Figure 3 shows the enhancement in indentation modulus for nanocomposites with polystyrene (PS) brush grafted SiO_2 nanoparticles dispersed within ∼96 kg/mol PS matrices.[17] Compared to ∼100 kg/mol monomodal brush systems with a graft density of 0.05 ch/nm^2, the bimodal brush systems, with a comparable long brush grafted at a graft density of ∼0.05 chains/nm^2 and a short brush of ∼7 kg/mol at ∼0.2 graft density, demonstrate significantly improved dispersion.[36] In addition, the indentation modulus of the bimodal system is higher than both the

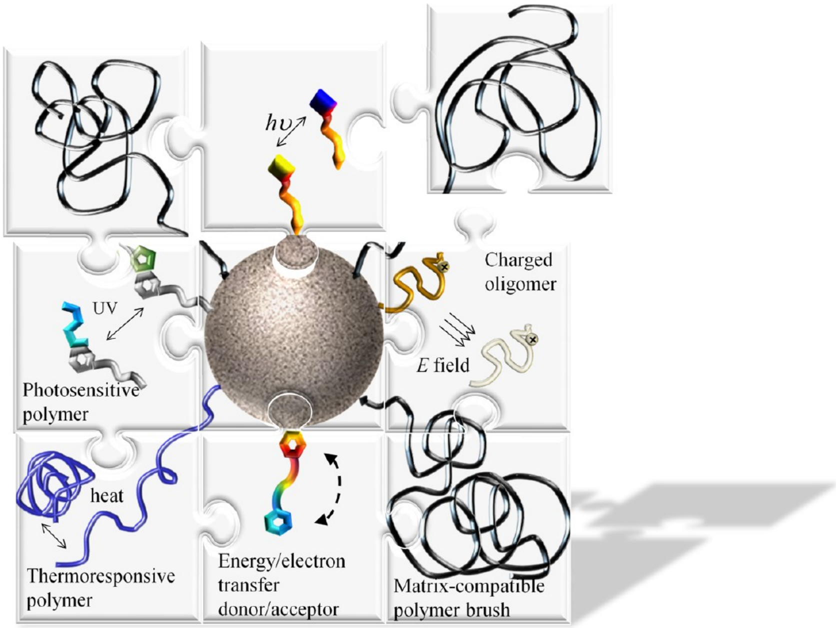

Figure 5. "Jigsaw puzzle" of the types of surface engineered molecules that could potentially be pieced together on a nanoparticle for optoelectronic applications.

composites with the monomodal brush modified particles and typical theoretical predictions.[17,36] This indicates that bimodal modification improves the dispersion and leads to matrix/brush entanglement and consequently strong filler matrix mechanical interaction.

The next level of complexity in surface ligand engineering is a polymer brush containing two chemically distinct species. These are mixed brushes, and extensive research based on mixed brushes grafted to flat or curved substrates has been carried out with a focus on environmental responsiveness to solvent conditions.[7,42−44] A mixed bimodal brush combines the desirable features of both bimodal and mixed brushes. It consists of two chemically distinct polymer brush species with significantly different molecular weights covalently tethered to the surface of nanofillers. The long brush plays a critical role in achieving good nanofiller dispersion when the short brush is enthalpically incompatible with the polymer matrix. Figure 4 shows results from our group for a model system of SiO_2 nanoparticles densely grafted with PS short brush and sparsely grafted with poly(methyl methacrylate) (PMMA) long brush. Good dispersion of nanoparticles was obtained in a PMMA matrix, which is chemically identical to the long brush while incompatible with the short brush. In contrast, spherical agglomeration of grafted nanoparticles was observed within a PS matrix, where the PMMA long brush collapses onto the nanoparticle surface to avoid contact with the PS matrix. Interestingly, good nanofiller dispersion did not deteriorate at higher matrix to brush molecular weight ratios, in spite of diminishing brush/matrix entanglement. It can be expected that a mixed multimodal brush can provide an opportunity to add functionality (using the short brush) while maintaining control over dispersion (using the long brush). Ironically, it is the complexity of multimodal surface ligand engineering that can simplify situations where matrix-incompatible functional groups need to be introduced into the system, and expand the choices of nanofillers, matrices, and the surface ligand chemistry that can be used to optimize properties.

Computation and theory have been important in guiding the design of nanoparticle brushes for use in both colloids and polymer matrices. Early work, including scaling models based on simple free energy balancing[45−47] and self-consistent field theory (SCFT) lattice models,[48−52] focused on analytically describing the brush equilibrium conformation (i.e., brush height and segment density distribution) and effective interactions between grafted surfaces under solvent conditions. Scaling models,[53,54] SCFT,[28,55−58] density functional theory (DFT),[59,60] and the polymer reference interaction site model (PRISM)[33,61,62] have elucidated the effect of the brush chain length, graft density, polydispersity, and chemistry on the brush wetting/dewetting behavior in a polymer matrix, interaction potential between grafted nanoparticles, and the resulting morphology of nanocomposites. Although many models have focused on situations where the grafted polymer is chemically identical to the matrix polymer,[33,56,57,63−65] there are a few that have handled the complexity of mixed polymer brushes.[66,67] An in depth discussion is outside the immediate scope of this paper, but a comprehensive summary of modeling and theory studies can be found in a number of excellent reviews.[27,68−72]

■ OPTOELECTRONIC APPLICATIONS

Surface ligand engineering has exciting implications for advanced optoelectronic applications. For example, theoretically we can take the various complexities described above and piece them together to create a polymer nanocomposite that is flexible and transparent, with both high refractive index and color conversion capability, and that reversibly responds to external stimuli such that the spatial distribution or extent of the optoelectronic properties can be dynamically controlled by an electric field or temperature (Figure 5). In the simplest case, taking advantage of the intrinsic properties of the fillers (such as nanoscale size to limit light scattering and suitable crystalline phase for high refractive index) and polymer matrices (such as flexibility, good processability, and transparency) still requires good nanofiller dispersion.[5,73−75] Given the refractive index mismatch (and thus enthalpic incompatibility) of filler and

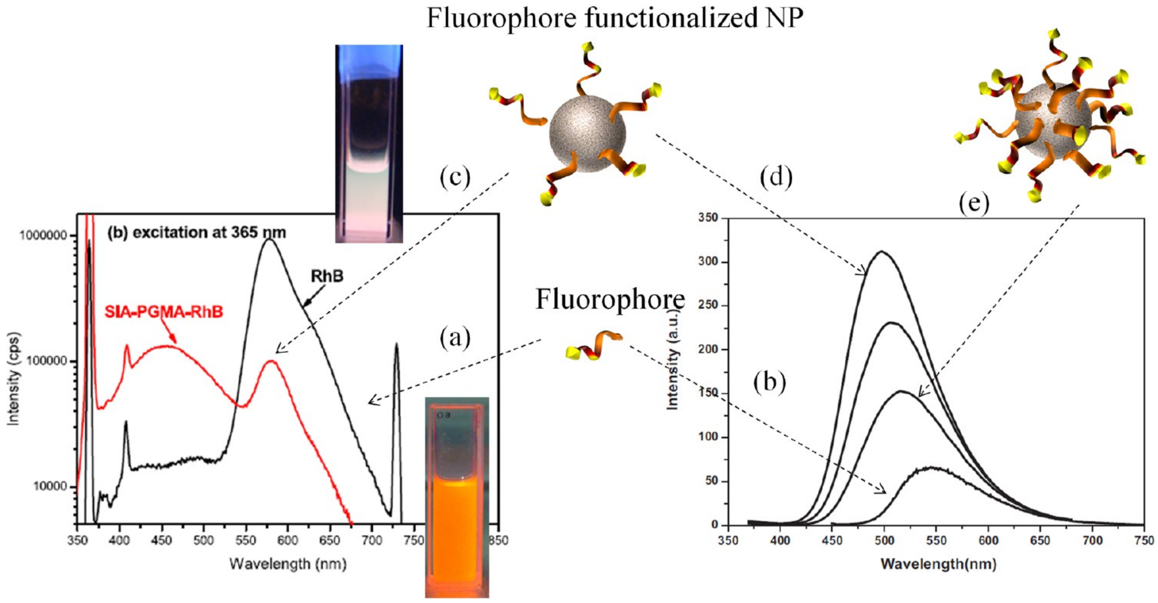

Figure 6. PL spectra showing how the attachment of an organic fluorophore ligands influences the fluorescent emission of functionalized nanoparticles.[77,88] (a) Rhodamine B (RhB) fluorophore; (b) Zn(MQ)$_2$ complex (MQ: 5-(2-methacryloylethyloxymethyl)-8-quinolinol); (c, d) corresponding fluorophore-functionalized nanoparticles to a and b; (e) functionalized nanoparticles suffering from concentration-quenching due to a higher graft density. Inset: digital photo for the a and c solution, respectively, where white light photoluminescence was obtained through mixing of yellow and blue emissions. Reproduced with permission from ref 77 (copyright 2008 Wiley−VCH) and ref 88 (copyright 2008 IOP Publishing).

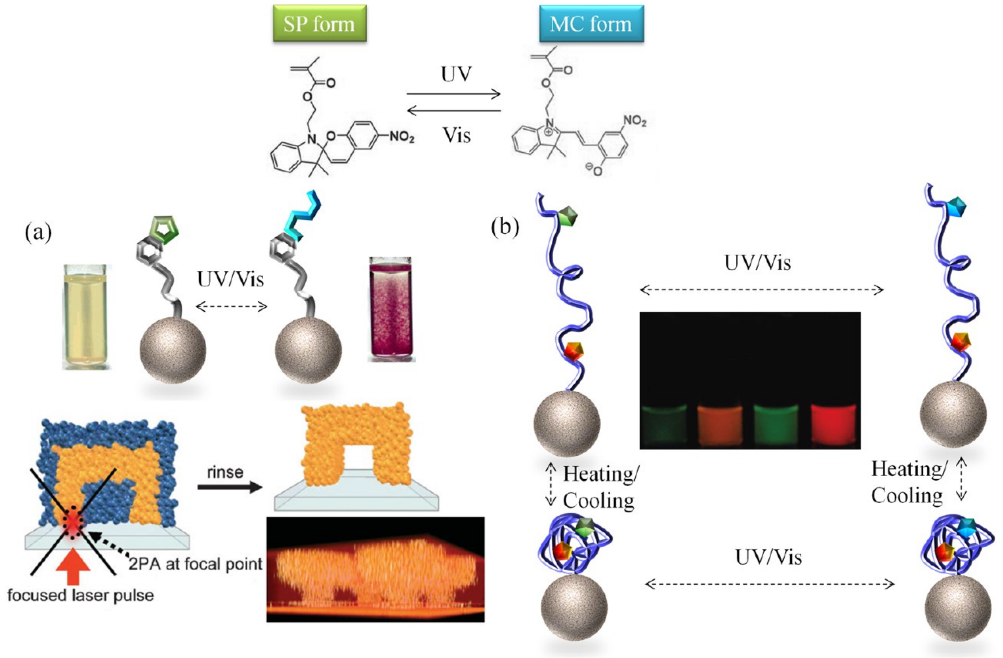

Figure 7. Photoswitching of surface ligands with a spirobenzopyran (SP) group to the fluorescent merocyanine (MC) form for use in direct laser writing[80,81] and switchable multicolor luminescent systems.[90] (a) Phototriggered aggregation and sedimentation behavior of SP-functionalized SiO$_2$ colloidal particles and their patterning process for 3D porous microscale structures. Inset: reflectance-mode confocal microscopy image of self-supported mushroom structure. (b) Thermoresponsive polymer brush with inner and outer layers of the brush selectively labeled with fluorescence resonance energy transfer (FRET) donors and photoswitchable acceptors. The FRET process can be controlled by UV/visible light irradiation, meanwhile thermo-induced collapse/swelling of the thermoresponsive PNIPAM gives rise to another level of modulation of the FRET efficiency by tuning spatial distances between fluorescent donors and acceptors. Reproduced with permission from ref 80 (Copyright 2009 Wiley-VCH), ref 81 (copyright 2006 American Chemical Society), and ref 90 (copyright 2009 American Chemical Society).

matrix, surface ligand engineering is essential. It could be as simple as a single population of chains with functional groups,[76−84] or a bimodal population of chains that maintain good dispersion of the filler within the matrix[17,18,34,36] or as complex as adding multiple functionalities while still using long chain ligands to ensure matrix compatibility.[85] These additional functionalities could include: photoluminescence, stimulus-responsiveness, energy conversion and storage, etc.

2.1. Dispersion in Solvents.

Extensive studies on functionalizing nanoparticles using surface ligand engineering have been completed on solvent suspensions or hybrid nanoparticle/solvent mixture systems. As a means for introducing photoluminescence for various applications such as luminescent tags, display planes, light emitting devices, etc.,[75,86,87] the use of rare-earth compound nanocrystals can be replaced with surface ligands containing fluorescent organic compounds. The surface-functionalized nanoparticles give fluorescent emission that can be tuned without changing the intrinsic crystal structure and size of the nanoparticles,[76,88] or provide mixed light of different wavelengths split from only one fluorophore emission (Figure 6).[77] The functionalized nanoparticles can further react with a range of substrates/surfaces to create fluorescent labeled objects.[78]

Another desired feature of optoelectronic materials is stimulus-responsiveness, which leads to many potential applications in sensors, optical switching, optical recording, pattern formation, and other photomodulated devices.[79−82,89] Functional units or polymer brushes that are responsive to the change of light, temperature, solvent quality, or electric field could be incorporated into the surface ligand systems. This approach has proven useful in manipulating the ligand conformational transformations to (1) modulate nanoparticle solubility in organic solvents,[89] (2) direct colloidal deposition onto photoswitchable substrate regions,[79,80] (3) interfere with other molecular functionalities integrated on the nanoparticle, such as switching of the fluorescence resonance energy transfer (FRET) process, to provide additional levels of modulation of the FRET efficiency (Figure 7).[90−92] In addition, the diversity of the surface ligand engineering toolbox allows optimization of nanoparticle/ligand interactions, such as energy and electron transfer processes from a surface-bound dye to the nanoparticle conduction band, leading to potential applications in light harvesting and photovoltaic solar cells.[93,94] Solar cell efficiency, which is largely determined by the efficiency of excited-state electron transfer process from a sensitizer dye to a semiconductor nanoparticle surface, could be tuned by varying the distance and anchoring orientation of the dye unit with respect to the nanoparticle surface.[95]

2.2. Dispersion in Polymer Matrices. Another key piece of the puzzle after functionalization, however, is dispersion of the functionalized nanoparticles into polymeric matrices. This is important not only for realizing the processability and commercialization of the optoelectronic materials, but also for taking advantage of the intrinsic properties of filler and matrix materials.[5,96,97] Flexible high-refractive-index optoelectronic materials with high optical transparency can be obtained by uniformly dispersing high-refractive-index nanoparticles such as TiO_2 or ZrO_2 into processable transparent polymer matrices,[98] leading to widespread applications including optical adhesives, encapsulants for light-emitting diode devices (LEDs), antireflective coatings, polarizers, optical data storages, and optical waveguides, etc.[35,73,98−103] The biggest challenge in dispersing high-refractive-index nanofillers in polymer matrices lies in their strong enthalpic incompatibility.[5] Success has been achieved in in situ incorporation of nanoparticles,[76,88,104] or homogeneous dispersion of nanoparticles in low molecular weight polymer matrix,[105] where the strongly bound matrix-compatible surface ligands not only markedly diminish the specific surface energy mismatch but also readily interpenetrate with short matrix chains to suppress autophobic dewetting. However, optimizing the optical properties of polymer nanocomposites requires both a high volume fraction of nanofiller, for greater property enhancement, and high molecular weight of matrix, for better mechanical integrity. In this case, conventional attempts to use a single population of surface ligands to control nanoparticle dispersion are challenged by a dilemma between the need for high graft density to reduce particle core/core attractions and the need for low graft density to reduce the entropic penalty for matrix penetration into the brush.[24,25,106] Dispersing a large volume fraction of nanoparticles with a large surface energy mismatch into a bulk polymer matrix was successfully achieved using bimodal brush surface ligand engineering leading to mm-thick transparency polymer nanocomposites for LED encapsulants, as shown in Figure 8b.[18,34]

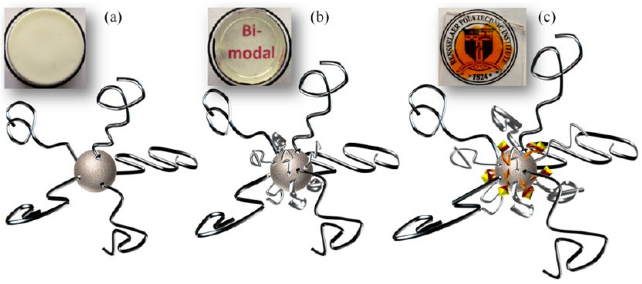

Figure 8. Comparison of the transparency (which is critically dependent on dispersion) between (a) monomodal, (b) bimodal, and (c) mixed multimodal brush modified nanoparticle/silicone nanocomposites.[18,85] Reproduced with permission from ref 18 (copyright 2013 American Chemical Society) and ref 85 (copyright 2013 Cambridge University Press).

2.3. Added Functionality and Controlled Dispersion. Putting together the pieces of the puzzle, we can also create functionalized nanoparticles and disperse them. Earlier work attempting to simultaneously introduce functionality and matrix compatibility onto nanoparticle surfaces was achieved with a polymeric ligand system containing a robust anchor, a functional molecule, and a group that increased the solubility of the nanoparticles in organic solvents tailored for various potential applications.[107] For ex-situ preparation of bulk polymer nanocomposites, surface functionalities typically do not protect the nanoparticles against agglomeration. Thus, in order to have independent control over functionality and matrix compatibility, a mixed-multimodal-brush approach is more powerful. In a notable example, yellow-emitting organic phosphor molecules with suitable anchoring groups were attached onto bimodal brush grafted ZrO_2 nanoparticles.[85] The matrix-compatible bimodal brushes ensure homogeneous dispersion of the nanoparticle within high molecular weight commercial silicone matrix, as shown in Figure 8c; meanwhile the phosphor ligands offer tunable photoluminescence properties of the nanocomposites in terms of (1) the robust anchoring of organic fluorescent group effectively reduces nonradiative quenching and therefore gives more efficient fluorescent emission; (2) the phosphor intermolecular spacing can be controlled by the mixed-multimodal-brush design including varying the graft density and volume fraction of each brush population, as well as the loading fraction of functionalized nanofillers. The obtained high-refractive-index nonscattering color-conversion silicone nanocomposite is a promising candidate for white LED encapsulation.[85] As a proof-of-concept trial, we created a similar mixed-multimodal-brush modified ZrO_2/silicone system. With optimized graft density of phosphor ligands ensuring highly efficient fluorescent emission, the functionalized nanoparticles were uniformly dispersed within silicone matrices at different loading fractions. The transparent hemispherical-shaped nanocomposites were excited with a blue LED and the resultant CIE color coordinates were measured to demonstrate the color-tuning capability of the nanocomposite, as shown in Figure 9.

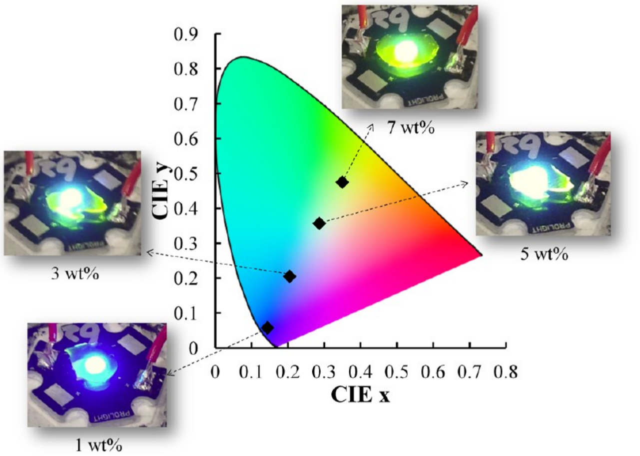

Figure 9. CIE *x*−*y* coordinates and corresponding digital photographs of a blue LED coated with silicone nanocomposites containing mixed-multimodal-brush modified ZrO_2/silicone nanoparticles at different loadings.

Looking forward, we envision even more complex nanocomposite systems. For example, to make a flexible, transparent, high-refractive-index, color-converting polymer nanocomposite with dynamically controllable properties, we can utilize mixed multimodal surface ligand engineering (Figure 10): long brushes grafted onto high-refractive-index nanoparticles at a relatively low graft density to tailor the entropic interaction and interparticle spacing, two shorter brush species with organic fluorescent groups and stimuli-responsive units, respectively, attached to introduce photoluminescence and external field mobility, and the residual grafting sites on the particle surface filled with a densely grafted short brush to tailor the particle core/core enthalpic interaction. The graft density and volume ratio of each brush species can be adjusted to prevent high-refractive-index nanoparticle agglomeration as well as promote more efficient fluorescent emission by localizing organic fluorescent groups in a manner that reduces nonradiative quenching. Such nanocomposites will offer exciting possibilities in advanced lighting applications such as dynamic optical control, including color mixing and beam shaping, of smart LED devices at the luminaire level. Mechanical integrity and the shape changing ability of the nanocomposite can be tailored by further introducing additional network-forming groups, as in an organogel, into the long brush chains, or adapting a suitable encapsulation material for dynamically adjustable shape and graded refractive index gradients for new levels of optical control in future lighting systems.

NANODIELECTRICS

The enhanced dielectric properties of nanofilled polymers have led to significant research in this field.[108−110] For example, the addition of nanoscale fillers to traditional insulating polymers has led to 50% improvements in dielectric breakdown strength and order of magnitude improvements in endurance strength.[108,111] Although the mechanisms leading to this improvement are still under investigation, the primary cause is likely related to carrier trapping and scattering at the nanofiller/matrix interface during the development of electronic avalanches. Nanocomposites have also exhibited both permittivity below and above that predicted theoretically, and in some cases, the permittivity can be increased without increasing the loss in frequencies of interest.[112] The tailorability of the dielectric constant is due to the high dielectric constant of some nanofillers, the ability of the nanofillers to alter local polymer chain mobility, morphology, and the local interfacial polarization that occurs or is introduced through surface ligands. Comparison of the effect of nanofiller dispersion on breakdown strength[113] and permittivity[114] as well as identification of electronically altered behavior of the matrix in the

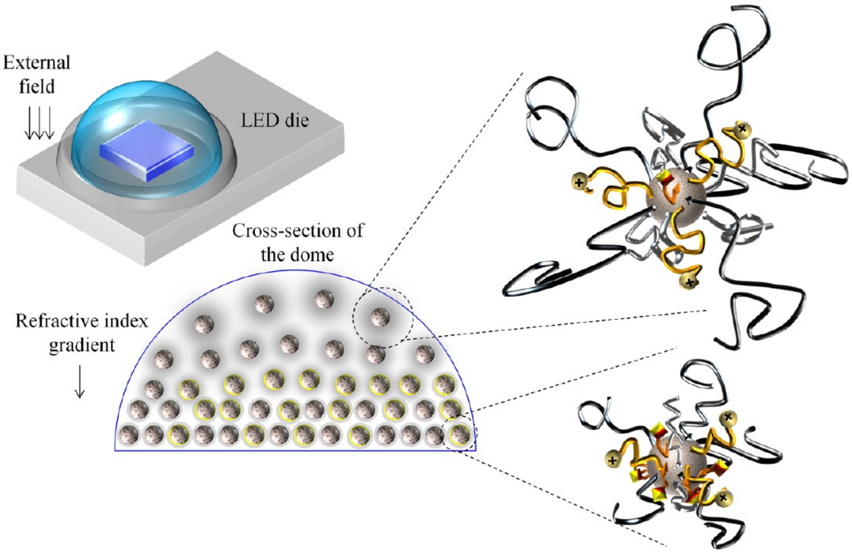

Figure 10. Schematic view of a nonscattering color-converting LED encapsulant with dynamically controllable refractive index gradient for advanced solid-state lighting applications. Graft density and volume fraction of each brush populations are adjusted for optimal color-converting efficiency and light extraction efficiency.

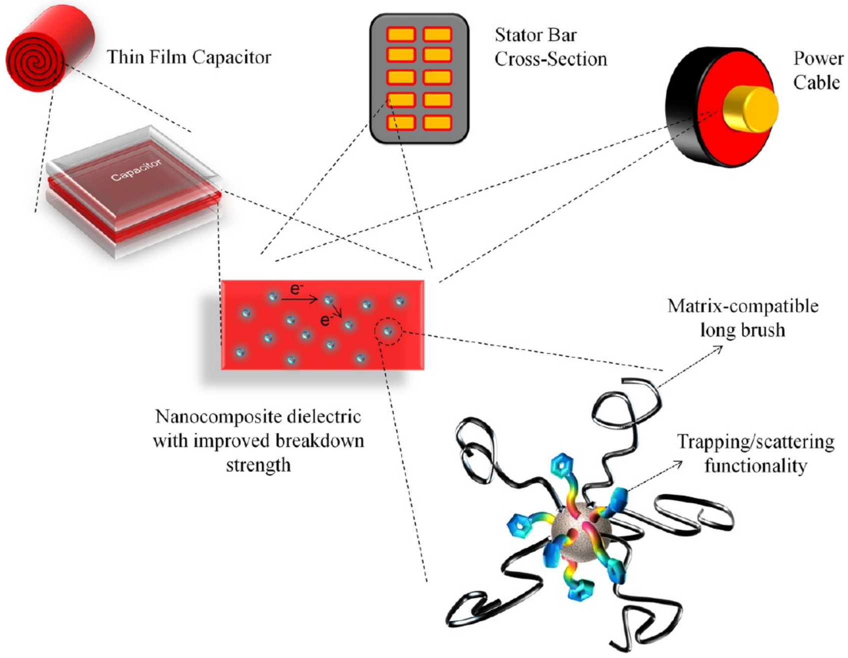

Figure 11. Schematic view of example dielectric applications critically dependent on breakdown strength. Composites utilizing mixed bimodal brush grafted filler particles comprised of long chains to control dispersion and short electronically functional chains for breakdown strength enhancement may revolutionize materials design for dielectrics.

region around the filler particles[115−117] singles out the matrix/filler interface as the critical feature in determining the dielectric properties of a nanocomposite.[118−121] Therefore, surface ligand engineering is a powerful means for tailoring the interface and thus dielectric properties that impact a variety of dielectric applications (Figure 11).

3.1. Dispersion in Polymer Matrices. Control over dispersion is critical to fully realizing the potential of the nanofiller interface to tailor the permittivity, breakdown strength, and endurance.[122] Poor dispersion will lead to agglomerates that induce the same deleterious effects as their micrometer-scale counterparts. Micrometer-scale defects cripple dielectric breakdown strength while increasing dielectric losses.[118,123−125] Additionally, because of the random nature of agglomeration, high-aspect-ratio asperities may be created, leading to significant local field concentrations, further reducing breakdown strength (though potentially increasing permittivity). Thus, at the very least, surface modification is required to control dispersion. This control has been achieved repeatedly through ligand engineering[42,126] and has been demonstrated directly in nanodielectrics, increasing breakdown strength by up to 50% through the reduction of agglomeration.[127−129] Challenges still exist, however, when nanoparticles with short molecule ligands have been scaled up for commercial use. Accordingly, the use of brushes, particularly in thermoplastics, should be more fully explored. The challenge here lies in the attachment of polymer brushes with the chemistry compatible with typical insulating materials such as olefins. It is also important to note that unlike in optical applications, random dispersion may not be the optimal mixing state. Though unstudied to date, semidisperse structures such as strings or sheets or fractal-like structures[130] may be the key to optimization permittivity and breakdown.[113] This level of control also requires the use of brushes. This is a relatively unexplored area ripe for optimization.

3.2. Altering Matrix Chain Mobility. Once dispersion has been achieved, a significant opportunity for surface ligand engineering is in altering the chain mobility in the interfacial region.[131] Reduction in matrix chain mobility reduces the permittivity.[132] In general, in systems where the matrix is strongly associated with the filler causing an increase in the glass transition temperature there will also be an accompanying decrease in permittivity.[133,134] Mobility can be reduced through polymer ligands that entangle with the matrix or short ligands that covalently bond with the matrix.[112] In addition, this decrease in mobility is accompanied by a reduction in free volume which is hypothesized to be a critical factor in increasing breakdown strength.[135] Covalent bonding of nanofillers to the matrix through cross-linkable functional groups is expected to reduce mobility and free volume and has been shown to be effective at increasing breakdown strength.[136,137] Mobility can also be altered through changes in the crystalline structure. All else being equal, crystalline regions have a lower permittivity and lower loss because of limited molecular mobility due to increased packing density.[138] Short molecules can alter the filler surface energy, which alters nucleation and growth[139−141] and thus the local crystalline morphology. These changes in crystalline morphology can impact both permittivity and breakdown strength through the same mechanisms discussed above.[142,143] This is also an area that deserves further exploration. An interesting alternative was demonstrated in ferroelectric polymers in which the crystalline regions are implicated as the primary source of their remarkable polarizability. The use of nanofillers to enhance crystallinity produced enhanced permittivity in these systems.[144,145] Percent crystallinity and crystallite size display significant effects on breakdown strength in polymers as well[146] and though not well studied as of yet, control over microstructure through the addition of nanofillers offers yet another knob for tuning dielectric properties. These morphological changes provide an interesting opportunity enhancing the dielectric strength and

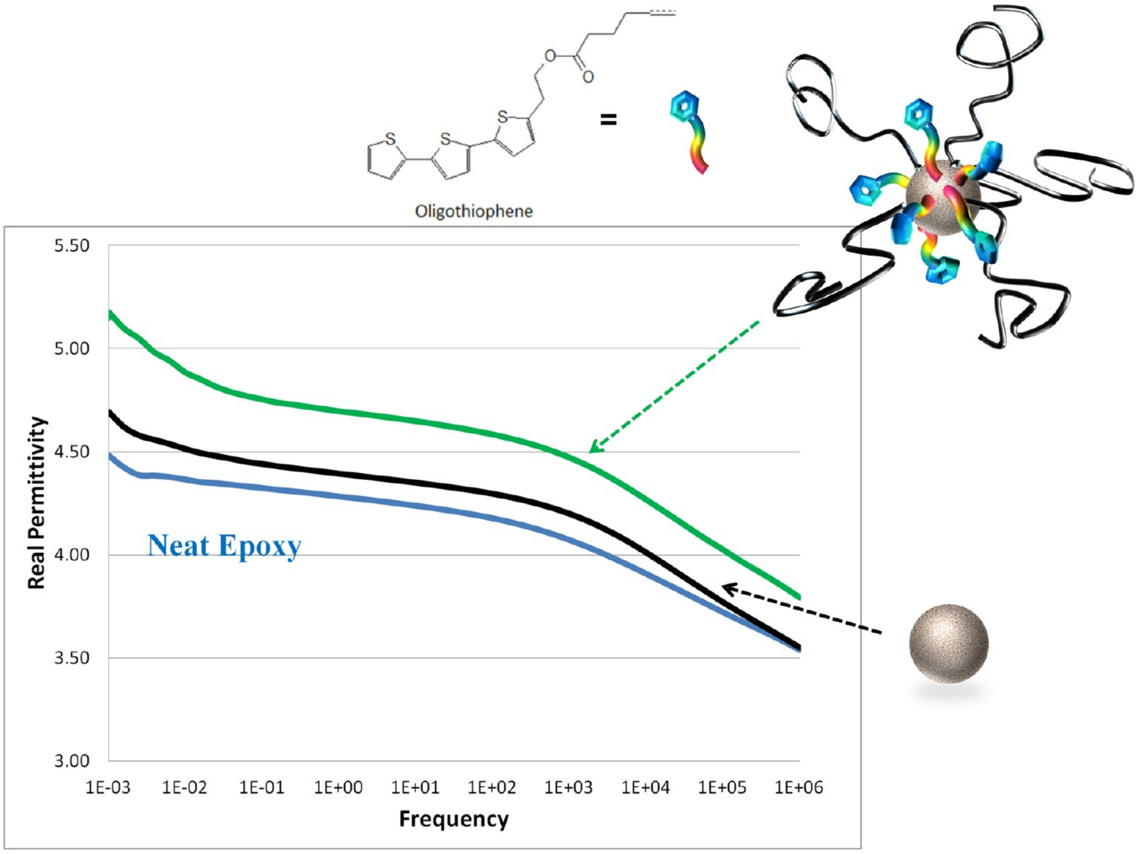

Figure 12. Real permittivity of an epoxy (bisphenol A diglycidyl ether based) and two SiO_2/epoxy nanoparticle composites, one with unmodified SiO_2 nanoparticle fillers, and one with mixed bimodal brush modified fillers (long chain: ~10 kg/mol polyglycidylmethacrylate for matrix-compatibility; short chain: trithiophene oligomers). SiO_2 nanoparticle fillers with mixed bimodal surface ligands drive composite permittivity higher than that of the base resin (shown) or SiO_2 (3.9).[149]

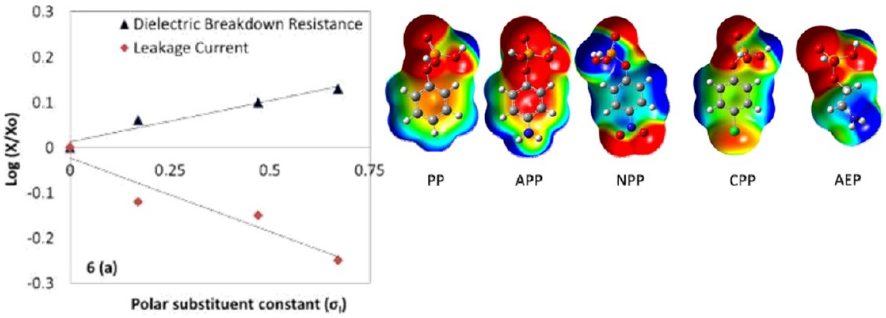

Figure 13. Comparing dielectric composite properties to polar Hammett constants of ligand molecules reveals dependence of bulk composite properties on interface chemistry.[152] Reproduced with permission from ref 152. Copyright 2013 American Chemical Society.

controlling permittivity in dielectric composites through ligand engineering.

3.3. Electronically Active Ligands. Polar groups can also be grafted to the nanofiller surface directly to enhance permittivity above the values predicted by traditional permittivity models.[147,148] In some cases, these groups may form due to a reaction with the filler surface,[147] but can also be tailored via coupling agents.[114] The challenge in this case is that the polar ligands can cause aggregation, again pointing to the need for more complex surface ligand design. One can envision an opportunity for bimodal ligand engineering in which the polarizabilty of the interface region is increased using a high density of short ligands and the interaction with the matrix is controlled using a low density of polymer brushes to either covalently link with the matrix or alter the local matrix morphology. Permittivity data from composites using this scheme of ligand architecture can be seen in Figure 12, where the composite is seen to display permittivity higher than the matrix or filler, or even the unmodified filler in composite.

Another interesting opportunity is the use of surface ligands to enhance electron trapping and or scattering, or even local conductivity. Electron trapping molecules at the surface of the nanofiller are theorized to be responsible for a reduction in average carrier mobility and energy in the polymer[150] and have been shown to provide substantial benefits to breakdown strength even at elevated temperature.[102,151] Selection of active groups which best induce additional trapping of electrons at the filler surface will further enhance surface scattering effects, and

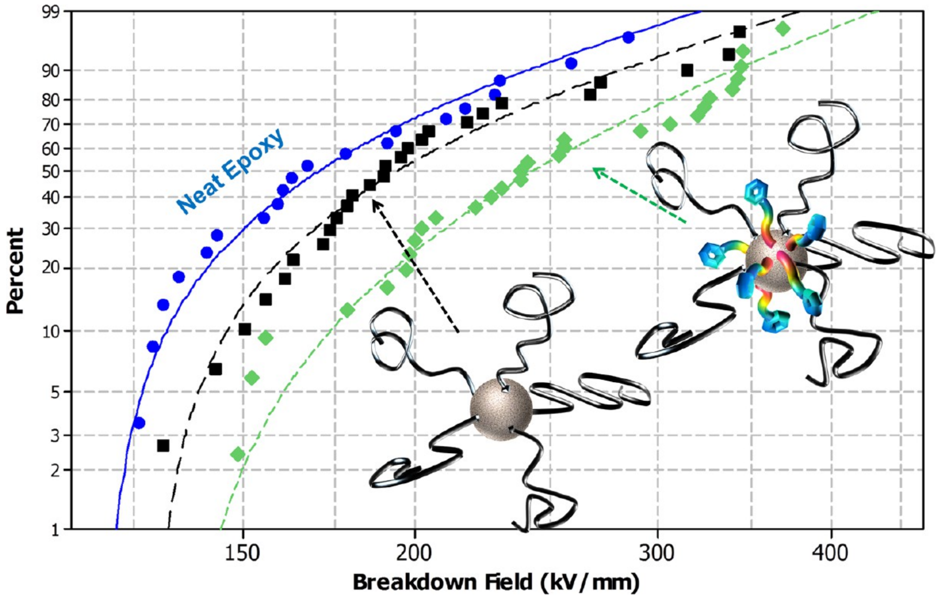

Figure 14. Weibull plots of dielectric breakdown for a neat epoxy and two SiO_2/epoxy nanoparticle composites, one with SiO_2 particles modified with a single population of matrix compatible chains, and one with mixed bimodal brush modified fillers. SiO_2 nanoparticle fillers with mixed bimodal surface ligands are show to increase breakdown strength over that of the neat epoxy or the composite with only matrix compatible chains.[149]

studies of the systematic variation of these surface properties are finally beginning to reveal the enormity of their implication for dielectric material design (see Figure 13).[152]

3.4. Added Functionality and Controlled Dispersion.

The challenge of the recent work on introducing electron trapping ligands is that the fillers agglomerated due to surface modification. To truly understand the effect of surface electrical behavior on permittivity and breakdown strength as well as control their interdependence, dispersion must be independently controlled through the creation of a mixed bimodal brush. The combination of good dispersion to maximize the available interface and tailoring interface properties to enhance trapping activity will provide a powerful two-prong strategy for enhancing breakdown strength in polymers. Recent work using mixed bimodal brush modified nanoparticle fillers has revealed that controlling both dispersion and surface chemistry can create improvements in AC breakdown strength greater than 40% at loadings as low as 2% (see Figure 14),[149] generating improvements greater than those seen with dispersion control or electroactive small molecules alone.

Further development of multimodal surface modification through ligand engineering will allow for the combination and tuning of multiple functionalities leading to materials with properties adjustable for specific dielectric applications. Other phenomena often implicated in insulation failure are water absorption leading to the development of water trees, the evolution of space charge under applied fields and field concentrations at defects. Surface chemistry has been shown to be capable of altering water absorption,[153−155] which could mitigate water tree formation. Surface chemistries that enhance local conductivity have been shown to limit space charge build up by allowing some relaxation of charge concentrations.[156−158] As space charge build up is implicated in insulation failure over time, this mitigation may substantially enhance insulation lifetime. Field concentrations could also be mitigated with field-dependent kinetic dissociation of stress grading molecules on particle surfaces, similar to that of tree-retardant grades of cross-linked polyethylene.[159] If ligands that cross-link upon exposure to internal partial discharges can be designed and grafted to the filler surface, a mechanism for limited self-healing in insulation could also be achieved. Multimodal surface modification's true strength is in permitting the isolation of particular properties of the interface while controlling for conflating parameters. In addition to the creation of multifunctional surface modified fillers for engineering solutions, fundamental mechanistic studies will benefit from this control. Ultimately, the multifunctionality of ligand engineered surfaces is only limited by synthetic chemistry and ambition, and virtually any combination of characteristics might be achievable with the appropriate populations of surface ligands. Designing materials precisely tailored across a wide range of properties is a tantalizing goal, and is likely the next step in the advancement of spherical nanocomposite engineering.

■ APPROACHES USED IN SURFACE LIGAND ENGINEERING

4.1. Surface Grafting Chemistry.

Generally, surface ligand engineering includes two strategies, namely "grafting from" and "grafting to". In the "grafting to" method, free molecules/polymers, containing functional groups, react with nanofiller surface functional groups to create a covalent linkage. Because of steric hindrance, the graft density depends on the molecular weight and flexibility of the molecules.

Silane coupling, phosphate coupling, and "click chemistry" can all be used for "grafting to" a variety of nanoparticles, such as TiO_2,[160] ITO,[161] and SiO_2.[9,162−165] Silane coupling has been widely reviewed.[165,166] More phosphate functional groups have been used to attach molecules to the surface of titania,[160,167] barium titanate.[168] In addition, the use of copper-catalyzed azide−alkyne cycloaddition ("click chemistry") has become a common tool for grafting to and can be used on polymers synthesized using a variety of methods[9,160−164] because of the easy preparation of clickable blocks (alkyne and azido end-capped moieties) and high efficiency and specificity of the reaction. It does, however, leave a copper catalyst in the mixture.

One technique that can be used to tailor the brushes before attachment is reversible addition−fragmentation chain transfer (RAFT) polymerization which is adaptable to almost all radical polymerizable monomers. For example, it can be used to prepare alkyne and azido end-capped polymers for "click" reaction or through the use of a trimethoxysilane containing RAFT agent[165] to create a polymer that can couple to the hydroxyl groups common on metal oxide nanoparticles. Atom transfer radical polymerization (ATRP)[166] was also used to graft a previously prepared triblock copolymer to silicon wafers.

In the "grafting from" method, polymerization is initiated on the nanofiller surface and the polymer grows in situ. This technique can generate a relatively high graft density due to the absence of steric hindrance. A variety of controlled radical polymerizations (CRP), such as ATRP, nitroxide-mediated polymerization (NMP) and RAFT, have been employed to graft a wide range of polymers from surfaces over a broad range of graft densities.[163,169−181] These methods have been reviewed by Benicewicz,[182] Brittain,[183] Matyjaszewski,[184,185] and Perrier.[186]

Recently, nanofillers with bimodal polymer brushes have been developed to decrease the entropic interfacial tension between the grafted and the matrix polymer brushes, and suppress dewetting in polymer matrices.[167] There are only a few reports on the preparation of bimodal brush grafted surfaces. Minko et al.[187] grafted two incompatible polymer brushes, carboxyl-terminated polystyrene and poly(2-vinylpyridine), to silicon wafer consecutively via a "grafting to" technique. Zhao and He[188] reported using a surface anchored "Y" shaped initiator to consecutively conduct ATRP and NMP for grafting poly(acrylic acid) and polystyrene mixed bimodal brushes on silicon wafer. Benicewicz et al.[36] first reported preparing bimodal polymer brushes on small size SiO_2 nanoparticles (diameter <100 nm), which is significant for polymer nanocomposites because bimodal brushes had previously only been grafted on silicon wafer or 150 nm SiO_2 particles. The synthesis was based on consecutive RAFT polymerizations. The original SiO_2 nanoparticles were reacted with 3-aminopropyldimethylethoxysilane to form amino functionalized SiO_2 nanoparticles followed by the reaction with mercaptothiazoline-activated RAFT agent (CPDB) to obtain RAFT agent coated nanoparticles. After the first surface-initiated RAFT polymerization, the terminal dithiobenzoate moiety was removed by treating with excess amount of AIBN. The exact surface chemistry was repeated one more time to obtain a second population of polymer brushes. This synthesis strategy can be widely employed to prepare bimodal homopolymer brushes and mixed brushes on surfaces including PS/PMMA, PS/PS, and PMMA/PMMA (1st population/2nd population of polymers).

4.2. Ligand Exchange Process. For some nanofillers, such as TiO_2, ITO, and CdSe quantum dots (QDs), ligand exchange is an important strategy to prepare polymer brushes that are firmly attached to the nanoparticles. In this process, weakly bound molecules are replaced by molecules that can strongly bond to enhance the interactions between surface attached polymers and substrates. Oleic acid has been used as an important and common ligand in the synthesis of many metal oxide nanoparticles. It is quite helpful to stabilize the nanoparticles and improve the dispersity in some organic solvents. However, oleic acid is a weak binder and is usually replaced with a silane agent[189] and phosphonic acid/phosphate[34,160,161,167,190] moiety to obtain stronger binding. A wide variety of surfaces, such as TiO_2,[160,167] ITO,[161] QDs,[34] iron oxide nanoparticles,[189,191−193] and nanocrystals,[194−203] have been modified via ligand exchange process.

4.3. Characterization of Surface Ligand Engineering. The characterization of ligand-functionalized nanoparticles is critically important for nearly all applications, with particular emphasis on the nanoparticle−ligand binding and surface chain characteristics with monomodal, bimodal, mixed bimodal, and multimodal distributions. There are several factors that need to be well-characterized in surface ligand engineering. The first one is graft density. A variety of small molecule ligand-functionalized nanoparticles have been analyzed using their unique UV−vis and/or IR absorptions.[181,204] The number of small molecules bound to the surface can be measured quantitatively based on the comparison between the absorbance of ligand functionalized particles and a standard UV−vis absorption curve plotted from known concentrations of free ligands. The graft density of polymer grafted nanoparticles can be determined by TGA when the polymer brushes have a narrow length distribution. The second factor is grafting distributions. The polymer length distribution can be easily characterized by GPC analysis of cleaved polymer chains. However, the characterization of spatial distribution of the brushes on particle surfaces is not easy. Recently, significant progress has been achieved in characterization of spatially symmetric and asymmetric distribution of surface functionalities.[8,205,206] TEM so far is the main technique to qualitatively characterize the asymmetric distribution of surface functionalities.[207−212] The third factor is the morphology of surface grafted brushes. The specific morphology of the brushes is affected by the interactions between the brush and the dispersion solvent or polymer matrix. The dimensions of the brush have been characterized by dynamic light scattering accompanied by theory and simulation.[213−220] In benign solvents, the nanoparticle-attached spherical brush morphology agrees with the dimensions of free chains in the same solvents.[221] In polymer matrices, small-angle neutron scattering (SANS) accompanied with selective labeling demonstrated that there is a significant reduction of the brush dimensions in polymer matrices compared to typical organic solvents.[222] Kumar et al.[223] recently specifically discussed the characterization of nanoparticle-attached brush structures in organic solvents and polymer matrices. Recently, the characterization of surface ligand engineering of polymer nanocomposites has been reviewed by Kumar,[223] Koo,[224] Mittal,[225] and Hussain.[3]

■ SUMMARY

Surface ligand engineering has been promoting the rapid evolution of nanocomposites, from compatibilizing inorganic nanofillers with an organic matrix to introducing tunable functionalities in addition to the intrinsic properties of nanofiller and matrix. The earliest use of surface ligand engineering includes stabilization of nanofillers in solvent suspensions, where the enthalpic-driven aggregation can be readily counterbalanced. The stable solvent suspensions later offer exciting opportunities for post functionalization of nanoparticles with functional surface ligands, which can be composed of a single ligand species or mixed ligands with different functionalities or environmental responsiveness. Polymer nanocomposite systems, on the other hand, possess more complex enthalpic and entropic nanofiller/matrix interactions, and therefore have a narrower window for good dispersion of nanofillers. Compared to a single population of matrix-compatible polymer brushes, where the enthalpic and entropic interactions are coupled, a bimodal brush system has proven to expand the dispersion window by decoupling the efforts on enthalpically screening core/core attraction and entropically facilitating brush/matrix interpenetration. Adding another level of complexity to the polymer nanocomposite, a multimodal brush system provides not only highly integrated functionalities but also good matrix compatibility, leading to more innovative solutions to widespread applications.

AUTHOR INFORMATION

Corresponding Author

*E-mail: schadl@rpi.edu. Tel.: (518) 276-2022. Fax: (518) 276-8554.

Notes

The authors declare no competing financial interest.

ACKNOWLEDGMENTS

This work was supported primarily by the Engineering Research Centers Program (ERC) of the National Science Foundation under NSF Cooperative Agreement EEC-0812056 and in part by New York State under NYSTAR contract C090145 and NSF (BME 1032579). The authors also acknowledge the financial support from the Nanoscale Science and Engineering Initiative of the National Science Foundation under NSF Award DMR-0642573, and ABB Corporate Research. We thank Atri Rungta and Michael Bell for preparing mixed-bimodal-brush samples, and Prolight Opto Technology Corporation for providing uncapped LEDs. The authors also thank Robert F. Karlicek, Jr., Keith Nelson, Chaitanya Ullal, Henrik Hillborg, and Su Zhao for inspiring discussions. In particular, Robert F. Karlicek, Jr. gave many detailed remarks that helped to refine our thinking.

REFERENCES

(1) Schaefer, D. W.; Ryan, S. How Nano Are Nanocomposites? *Macromolecules* **2007**, *40*, 8501−8517.

(2) Kumar, S. K.; Krishnamoorti, R. Nanocomposites: Structure, Phase Behavior, and Properties. *Annu. Rev. Chem. Biomol. Eng.* **2010**, *1*, 37−58.

(3) Hussain, F.; Hojjati, M.; Okamoto, M.; Gorga, R. E. Review Article: Polymer-Matrix Nanocomposites, Processing, Manufacturing, and Application: An Overview. *J. Compos. Mater.* **2006**, *40*, 1511−1575.

(4) Krishnamoorti, R.; Vaia, R. A. Polymer Nanocomposites. *J. Polym. Sci., Part B: Polym. Phys.* **2007**, *45*, 3252−3256.

(5) Caseri, W. Nanocomposites of Polymers and Metals or Semiconductors: Historical Background and Optical Properties. *Macromol. Rapid Commun.* **2000**, *21*, 705−722.

(6) Zhao, B.; Brittain, W. J. Polymer Brushes: Surface-Immobilized Macromolecules. *Prog. Polym. Sci.* **2000**, *25*, 677−710.

(7) Zhao, B. Synthesis of Binary Mixed Homopolymer Brushes by Combining Atom Transfer Radical Polymerization and Nitroxide-Mediated Radical Polymerization. *Polymer* **2003**, *44*, 4079−4083.

(8) Lattuada, M.; Hatton, T. A. Synthesis, Properties and Applications of Janus Nanoparticles. *Nano Today* **2011**, *6*, 286−308.

(9) Li, J.; Wang, L.; Benicewicz, B. C. Synthesis of Janus Nanoparticles Via a Combination of the Reversible Click Reaction and "Grafting to" Strategies. *Langmuir* **2013**, *29*, 11547−11553.

(10) Marko, J. F. Polymer Brush in Contact with a Mixture of Solvents. *Macromolecules* **1993**, *26*, 313−319.

(11) Brown, H. R.; Char, K.; Deline, V. R. Enthalpy-Driven Swelling of a Polymer Brush. *Macromolecules* **1990**, *23*, 3383−3385.

(12) Dutta, N.; Green, D. Nanoparticle Stability in Semidilute and Concentrated Polymer Solutions. *Langmuir* **2008**, *24*, 5260−5269.

(13) Taunton, H. J.; Toprakcioglu, C.; Fetters, L. J.; Klein, J. Interactions between Surfaces Bearing End-Adsorbed Chains in a Good Solvent. *Macromolecules* **1990**, *23*, 571−580.

(14) Green, P. F. The Structure of Chain End-Grafted Nanoparticle/Homopolymer Nanocomposites. *Soft Matter* **2011**, *7*, 7914−7926.

(15) Stamm, M.; Sommer, J. U. Polymer-Nanoparticle Films: Entropy and Enthalpy at Play. *Nat. Mater.* **2007**, *6*, 260−261.

(16) Balazs, A. C.; Emrick, T.; Russell, T. P. Nanoparticle Polymer Composites: Where Two Small Worlds Meet. *Science* **2006**, *314*, 1107−1110.

(17) Natarajan, B.; Neely, T.; Rungta, A.; Benicewicz, B. C.; Schadler, L. S. Thermomechanical Properties of Bimodal Brush Modified Nanoparticle Composites. *Macromolecules* **2013**, *46*, 4909−4918.

(18) Li, Y.; Tao, P.; Viswanath, A.; Benicewicz, B. C.; Schadler, L. S. Bimodal Surface Ligand Engineering: The Key to Tunable Nanocomposites. *Langmuir* **2013**, *29*, 1211−1220.

(19) Pryamtisyn, V.; Ganesan, V.; Panagiotopoulos, A. Z.; Liu, H.; Kumar, S. K. Modeling the Anisotropic Self-Assembly of Spherical Polymer-Grafted Nanoparticles. *J. Chem. Phys.* **2009**, *131*, 221102.

(20) Alexander, S. Polymer Adsorption on Small Spheres−Scaling Approach. *J. Phys. (Paris)* **1977**, *38*, 977−981.

(21) Alexander, S. Adsorption of Chain Molecules with a Polar Head−A Scaling Description. *J. Phys. (Paris)* **1977**, *38*, 983−987.

(22) de Gennes, P. G. Conformations of Polymers Attached to an Interface. *Macromolecules* **1980**, *13*, 1069−1075.

(23) Azzaroni, O. Polymer Brushes Here, There, and Everywhere: Recent Advances in Their Practical Applications and Emerging Opportunities in Multiple Research Fields. *J. Polym. Sci., Part A: Polym. Chem.* **2012**, *50*, 3225−3258.

(24) Zheng, L.; Xie, A. F.; Lean, J. T. Polystyrene Nanoparticles with Anionically Polymerized Polybutadiene Brushes. *Macromolecules* **2004**, *37*, 9954−9962.

(25) Sunday, D.; Ilavsky, J.; Green, D. L. A Phase Diagram for Polymer-Grafted Nanoparticles in Homopolymer Matrices. *Macromolecules* **2012**, *45*, 4007−4011.

(26) Hoy, R. S.; Grest, G. S. Entanglements of an End-Grafted Polymer Brush in a Polymeric Matrix. *Macromolecules* **2007**, *40*, 8389−8395.

(27) Hall, L. M.; Jayaraman, A.; Schweizer, K. S. Molecular Theories of Polymer Nanocomposites. *Curr. Opin. Solid State Mater. Sci.* **2010**, *14*, 38−48.

(28) Xu, J.; Qiu, F.; Zhang, H.; Yang, Y. Morphology and Interactions of Polymer Brush-Coated Spheres in a Polymer Matrix. *J. Polym. Sci., Part B: Polym. Phys.* **2006**, *44*, 2811−2820.

(29) Takai, C.; Fuji, M.; Takahashi, M. A Novel Surface Designed Technique to Disperse Silica Nano Particle into Polymer. *Colloids Surf., A* **2007**, *292*, 79−82.

(30) Milner, S.; Witten, T.; Cates, M. Effects of Polydispersity in the End-Grafted Polymer Brush. *Macromolecules* **1989**, *22*, 853−861.

(31) de Vos, W. M.; Leermakers, F. A. Modeling the Structure of a Polydisperse Polymer Brush. *Polymer* **2009**, *50*, 305−316.

(32) Dodd, P. M.; Jayaraman, A. Monte Carlo Simulations of Polydisperse Polymers Grafted on Spherical Surfaces. *J. Polym. Sci., Part B: Polym. Phys.* **2012**, *50*, 694−705.

(33) Martin, T. B.; Dodd, P. M.; Jayaraman, A. Polydispersity for Tuning the Potential of Mean Force between Polymer Grafted Nanoparticles in a Polymer Matrix. *Phys. Rev. Lett.* **2013**, *110*, 018301.

(34) Tao, P.; Li, Y.; Siegel, R. W.; Schadler, L. S. Transparent Luminescent Silicone Nanocomposites Filled with Bimodal Pdms-Brush-Grafted Cdse Quantum Dots. *J. Mater. Chem. C* **2013**, *1*, 86−94.

(35) Tao, P.; Li, Y.; Siegel, R. W.; Schadler, L. S. Transparent Dispensible High-Refractive Index ZrO_2/Epoxy Nanocomposites for LED Encapsulation. *J. Appl. Polym. Sci.* **2013**, *130*, 3785−3793.

(36) Rungta, A.; Natarajan, B.; Neely, T.; Dukes, D.; Schadler, L. S.; Benicewicz, B. C. Grafting Bimodal Polymer Brushes on Nanoparticles Using Controlled Radical Polymerization. *Macromolecules* **2012**, *45*, 9303−9311.

(37) Dan, N.; Tirrell, M. Effect of Bimodal Molecular Weight Distribution on the Polymer Brush. *Macromolecules* **1993**, *26*, 6467−6473.

(38) Skvortsov, A.; Gorbunov, A.; Leermakers, F.; Fleer, G. Long Minority Chains in a Polymer Brush: A First-Order Adsorption Transition. *Macromolecules* **1999**, *32*, 2004−2015.

(39) Kent, M.; Factor, B.; Satija, S.; Gallagher, P.; Smith, G. Structure of Bimodal Polymer Brushes in a Good Solvent by Neutron Reflectivity. *Macromolecules* **1996**, *29*, 2843−2849.

(40) Edgecombe, S.; Gardiner, J.; Matsen, M. Suppressing Autophobic Dewetting by Using a Bimodal Brush. *Macromolecules* **2002**, *35*, 6475−6477.

(41) Reiter, G.; Schultz, J.; Auroy, P.; Auvray, L. Improving Adhesion Via Connector Polymers to Stabilize Non-Wetting Liquid Films. *Europhys. Lett.* **1996**, *33*, 29.

(42) Zhao, B.; Zhu, L. Mixed Polymer Brush-Grafted Particles: A New Class of Environmentally Responsive Nanostructured Materials. *Macromolecules* **2009**, *42*, 9369−9383.

(43) Sidorenko, A.; Minko, S.; Schenk-Meuser, K.; Duschner, H.; Stamm, M. Switching of Polymer Brushes. *Langmuir* **1999**, *15*, 8349−8355.

(44) Stuart, M. A. C.; Huck, W. T.; Genzer, J.; Müller, M.; Ober, C.; Stamm, M.; Sukhorukov, G. B.; Szleifer, I.; Tsukruk, V. V.; Urban, M. Emerging Applications of Stimuli-Responsive Polymer Materials. *Nat. Mater.* **2010**, *9*, 101−113.

(45) Daoud, M.; Cotton, J. P. Star Shaped Polymers - a Model for the Conformation and Its Concentration-Dependence. *J. Phys. (Paris)* **1982**, *43*, 531−538.

(46) Ohno, K.; Morinaga, T.; Takeno, S.; Tsujii, Y.; Fukuda, T. Suspensions of Silica Particles Grafted with Concentrated Polymer Brush: Effects of Graft Chain Length on Brush Layer Thickness and Colloidal Crystallization. *Macromolecules* **2007**, *40*, 9143−9150.

(47) Ohno, K.; Morinaga, T.; Takeno, S.; Tsujii, Y.; Fukuda, T. Suspensions of Silica Particles Grafted with Concentrated Polymer Brush: A New Family of Colloidal Crystals. *Macromolecules* **2006**, *39*, 1245−1249.

(48) Dan, N.; Tirrell, M. Polymers Tethered to Curved Interfaces - a Self-Consistent-Field Analysis. *Macromolecules* **1992**, *25*, 2890−2895.

(49) Wijmans, C. M.; Zhulina, E. B. Polymer Brushes at Curved Surfaces. *Macromolecules* **1993**, *26*, 7214−7224.

(50) Gast, A. P. Structure, Interactions, and Dynamics in Tethered Chain Systems. *Langmuir* **1996**, *12*, 4060−4067.

(51) Wijmans, C. M.; Scheutjens, J.; Zhulina, E. B. Self-Consistent Field-Theories for Polymer Brushes - Lattice Calculations and an Asymptotic Analytical Description. *Macromolecules* **1992**, *25*, 2657−2665.

(52) Ball, R. C.; Marko, J. F.; Milner, S. T.; Witten, T. A. Polymers Grafted to a Convex Surface. *Macromolecules* **1991**, *24*, 693−703.

(53) Ferreira, P. G.; Ajdari, A.; Leibler, L. Scaling Law for Entropic Effects at Interfaces between Grafted Layers and Polymer Melts. *Macromolecules* **1998**, *31*, 3994−4003.

(54) Martin, J. I.; Wang, Z. G. Polymer Brushes - Scaling, Compression Forces, Interbrush Penetration, and Solvent Size Effects. *J. Phys. Chem.* **1995**, *99*, 2833−2844.

(55) Kim, J. U.; Matsen, M. W. Interaction between Polymer-Grafted Particles. *Macromolecules* **2008**, *41*, 4435−4443.

(56) Trombly, D. M.; Ganesan, V. Curvature Effects Upon Interactions of Polymer-Grafted Nanoparticles in Chemically Identical Polymer Matrices. *J. Chem. Phys.* **2010**, *133*, 154904.

(57) Xu, J.; Qiu, F.; Zhang, H.; Yang, Y. Morphology and Interactions of Polymer Brush-Coated Spheres in a Polymer Matrix. *J. Polym. Sci., Part B: Polym. Phys.* **2006**, *44*, 2811−2820.

(58) Borukhov, I.; Leibler, L. Enthalpic Stabilization of Brush-Coated Particles in a Polymer Melt. *Macromolecules* **2002**, *35*, 5171−5182.

(59) Xu, X.; Cao, D. Density Functional Theory for Adsorption of Colloids on the Polymer-Tethered Surfaces: Effect of Polymer Chain Architecture. *J. Chem. Phys.* **2009**, *130*, 164901.

(60) Ginzburg, V. V. Polymer-Grafted Nanoparticles in Polymer Melts: Modeling Using the Combined Scft−Dft Approach. *Macromolecules* **2014**, *46*, 9798−9805.

(61) Nair, N.; Jayaraman, A. Self-Consistent Prism Theory - Monte Carlo Simulation Studies of Copolymer Grafted Nanoparticles in a Homopolymer Matrix. *Macromolecules* **2010**, *43*, 8251−8263.

(62) Jayaraman, A.; Nair, N. Integrating Prism Theory and Monte Carlo Simulation to Study Polymer-Functionalised Particles and Polymer Nanocomposites. *Mol. Simul.* **2012**, *38*, 751−761.

(63) Hore, M. J.; Ford, J.; Ohno, K.; Composto, R. J.; Hammouda, B. Direct Measurements of Polymer Brush Conformation Using Small-Angle Neutron Scattering (Sans) from Highly Grafted Iron Oxide Nanoparticles in Homopolymer Melts. *Macromolecules* **2013**, *46*, 9341−9348.

(64) Smith, G. D.; Bedrov, D. Dispersing Nanoparticles in a Polymer Matrix: Are Long, Dense Polymer Tethers Really Necessary? *Langmuir* **2009**, *25*, 11239−11243.

(65) Martin, T. B.; Jayaraman, A. Identifying the Ideal Characteristics of the Grafted Polymer Chain Length Distribution for Maximizing Dispersion of Polymer Grafted Nanoparticles in a Polymer Matrix. *Macromolecules* **2013**, *46*, 9144−9150.

(66) Price, A. D.; Hur, S.-M.; Fredrickson, G. H.; Frischknecht, A. L.; Huber, D. L. Exploring Lateral Microphase Separation in Mixed Polymer Brushes by Experiment and Self-Consistent Field Theory Simulations. *Macromolecules* **2011**, *45*, 510−524.

(67) Hur, S. M.; Frischknecht, A. L.; Huber, D. L.; Fredrickson, G. H. Self-Consistent Field Simulations of Self-and Directed-Assembly in a Mixed Polymer Brush. *Soft Matter* **2011**, *7*, 8776−8788.

(68) Ganesan, V.; Jayaraman, A. Theory and Simulation Studies of Effective Interactions, Phase Behavior and Morphology in Polymer Nanocomposites. *Soft Matter* **2014**, *10*, 13−38.

(69) Jayaraman, A. Polymer Grafted Nanoparticles: Effect of Chemical and Physical Heterogeneity in Polymer Grafts on Particle Assembly and Dispersion. *J. Polym. Sci., Part B: Polym. Phys.* **2013**, *57*, 524−534.

(70) Zeng, Q.; Yu, A.; Lu, G. Multiscale Modeling and Simulation of Polymer Nanocomposites. *Prog. Polym. Sci.* **2008**, *33*, 191−269.

(71) Glotzer, S. C.; Paul, W. Molecular and Mesoscale Simulation Methods for Polymer Materials. *Annu. Rev. Mater. Res.* **2002**, *32*, 401−436.

(72) Ganesan, V.; Ellison, C. J.; Pryamitsyn, V. Mean-Field Models of Structure and Dispersion of Polymer-Nanoparticle Mixtures. *Soft Matter* **2010**, *6*, 4010−4025.

(73) Beecroft, L. L.; Ober, C. K. Nanocomposite Materials for Optical Applications. *Chem. Mater.* **1997**, *9*, 1302−1317.

(74) Fang, C. Y.; Liu, Y. L.; Lee, Y. C.; Chen, H. L.; Wan, D. H.; Yu, C. C. Nanoparticle Stacks with Graded Refractive Indices Enhance the Omnidirectional Light Harvesting of Solar Cells and the Light Extraction of Light-Emitting Diodes. *Adv. Funct. Mater.* **2012**, *23*, 1412−1421.

(75) Talapin, D. V.; Lee, J. S.; Kovalenko, M. V.; Shevchenko, E. V. Prospects of Colloidal Nanocrystals for Electronic and Optoelectronic Applications. *Chem. Rev.* **2009**, *110*, 389−458.

(76) Gao, J.; Lü, C.; Lü, X.; Du, Y. Aphen-Functionalized Nanoparticles-Polymer Fluorescent Nanocomposites Via Ligand Exchange and in Situ Bulk Polymerization. *J. Mater. Chem.* **2007**, *17*, 4591−4597.

(77) Liu, Y. L.; Wu, Y. H.; Hsu, C. Y. Direct White Light Photoluminescent Nanoparticles with One Fluorophore. *Nanotechnology* **2009**, *20*, 235704.

(78) Tsyalkovsky, V.; Klep, V.; Ramaratnam, K.; Lupitskyy, R.; Minko, S.; Luzinov, I. Fluorescent Reactive Core−Shell Composite Nanoparticles with a High Surface Concentration of Epoxy Functionalities. *Chem. Mater.* **2007**, *20*, 317−325.

(79) Piech, M.; Bell, N. S. Controlled Synthesis of Photochromic Polymer Brushes by Atom Transfer Radical Polymerization. *Macromolecules* **2006**, *39*, 915−922.

(80) George, M. C.; Mohraz, A.; Piech, M.; Bell, N. S.; Lewis, J. A.; Braun, P. V. Direct Laser Writing of Photoresponsive Colloids for

Microscale Patterning of 3d Porous Structures. *Adv. Mater.* **2009**, *21*, 66−70.

(81) Bell, N. S.; Piech, M. Photophysical Effects between Spirobenzopyran-Methyl Methacrylate-Functionalized Colloidal Particles. *Langmuir* **2006**, *22*, 1420−1427.

(82) Piech, M.; George, M. C.; Bell, N. S.; Braun, P. V. Patterned Colloid Assembly by Grafted Photochromic Polymer Layers. *Langmuir* **2006**, *22*, 1379−1382.

(83) Kim, D.; Kim, Y.; Cho, J. Solvent-Free Nanocomposite Colloidal Fluids with Highly Integrated and Tailored Functionalities: Rheological, Ionic Conduction, and Magneto-Optical Properties. *Chem. Mater.* **2013**, *25*, 3834−3843.

(84) Thomas, K. G.; Kamat, P. V. Chromophore-Functionalized Gold Nanoparticles. *Acc. Chem. Res.* **2003**, *36*, 888−898.

(85) Li, Y.; Tao, P.; Siegel, R. W.; Schadler, L. S. Multifunctional Silicone Nanocomposites for Advanced LED Encapsulation. *MRS Online Proc. Libr.* **2013**, 1547.

(86) Bonaccorso, F.; Sun, Z.; Hasan, T.; Ferrari, A. Graphene Photonics and Optoelectronics. *Nat. Photonics.* **2010**, *4*, 611−622.

(87) Mao, A.; Karlicek, R. F. Surface Patterning of Nonscattering Phosphors for Light Extraction. *Opt. Lett.* **2013**, *38*, 2796−2799.

(88) Lü, C.; Gao, J.; Fu, Y.; Du, Y.; Shi, Y.; Su, Z. A Ligand Exchange Route to Highly Luminescent Surface-Functionalized Zns Nanoparticles and Their Transparent Polymer Nanocomposites. *Adv. Funct. Mater.* **2008**, *18*, 3070−3079.

(89) Raimondo, C.; Reinders, F.; Soydaner, U.; Mayor, M.; Samorì, P. Light-Responsive Reversible Solvation and Precipitation of Gold Nanoparticles. *Chem. Commun.* **2010**, *46*, 1147−1149.

(90) Wu, T.; Zou, G.; Hu, J.; Liu, S. Fabrication of Photoswitchable and Thermotunable Multicolor Fluorescent Hybrid Silica Nanoparticles Coated with Dye-Labeled Poly (N-Isopropylacrylamide) Brushes. *Chem. Mater.* **2009**, *21*, 3788−3798.

(91) Li, C.; Hu, J.; Liu, S. Engineering Fret Processes within Synthetic Polymers, Polymeric Assemblies and Nanoparticles Via Modulating Spatial Distribution of Fluorescent Donors and Acceptors. *Soft Matter* **2012**, *8*, 7096−7102.

(92) Li, C.; Zhang, Y.; Hu, J.; Cheng, J.; Liu, S. Reversible Three-State Switching of Multicolor Fluorescence Emission by Multiple Stimuli Modulated Fret Processes within Thermoresponsive Polymeric Micelles. *Angew. Chem.* **2010**, *122*, 5246−5250.

(93) Listorti, A.; O'Regan, B.; Durrant, J. R. Electron Transfer Dynamics in Dye-Sensitized Solar Cells. *Chem. Mater.* **2011**, *23*, 3381−3399.

(94) Bang, J. H.; Kamat, P. V. Cdse Quantum Dot−Fullerene Hybrid Nanocomposite for Solar Energy Conversion: Electron Transfer and Photoelectrochemistry. *ACS Nano* **2011**, *5*, 9421−9427.

(95) Rochford, J.; Galoppini, E. Zinc (II) Tetraarylporphyrins Anchored to TiO_2, ZnO, and ZrO_2 Nanoparticle Films through Rigid-Rod Linkers. *Langmuir* **2008**, *24*, 5366−5374.

(96) Kango, S.; Kalia, S.; Celli, A.; Njuguna, J.; Habibi, Y.; Kumar, R. Surface Modification of Inorganic Nanoparticles for Development of Organic-Inorganic Nanocomposites—a Review. *Prog. Polym. Sci.* **2013**, *38*, 1232−1261.

(97) Li, S.; Lin, M. M.; Toprak, M. S.; Kim, D. K.; Muhammed, M. Nanocomposites of Polymer and Inorganic Nanoparticles for Optical and Magnetic Applications. *Nano Rev.* **2010**, *1*, 5214.

(98) Liu, J. G.; Ueda, M. High Refractive Index Polymers: Fundamental Research and Practical Applications. *J. Mater. Chem.* **2009**, *19*, 8907−8919.

(99) Srivastava, S.; Haridas, M.; Basu, J. Optical Properties of Polymer Nanocomposites. *Bull. Mater. Sci.* **2008**, *31*, 213−217.

(100) Sanchez, C.; Lebeau, B.; Chaput, F.; Boilot, J. P. Optical Properties of Functional Hybrid Organic−Inorganic Nanocomposites. *Adv. Mater.* **2003**, *15*, 1969−1994.

(101) Tao, P.; Li, Y.; Rungta, A.; Viswanath, A.; Gao, J.; Benicewicz, B. C.; Siegel, R. W.; Schadler, L. S. TiO_2 Nanocomposites with High Refractive Index and Transparency. *J. Mater. Chem.* **2011**, *21*, 18623−18629.

(102) Nelson, J. K.; Hu, Y. Nanocomposite Dielectrics-Properties and Implications. *J. Phys. D: Appl. Phys.* **2005**, *38*, 213−222.

(103) Lü, C.; Yang, B. High Refractive Index Organic−Inorganic Nanocomposites: Design, Synthesis and Application. *J. Mater. Chem.* **2009**, *19*, 2884−2901.

(104) Martinez, Y.; Retuert, J.; Yazdani-Pedram, M.; Cölfen, H. Transparent Semiconductor−Polymer Hybrid Films with Tunable Optical Properties. *J. Mater. Chem.* **2007**, *17*, 1094−1101.

(105) Lee, S.; Shin, H. J.; Yoon, S. M.; Yi, D. K.; Choi, J. Y.; Paik, U. Refractive Index Engineering of Transparent ZrO_2−Polydimethylsiloxane Nanocomposites. *J. Mater. Chem.* **2008**, *18*, 1751−1755.

(106) Meli, L.; Arceo, A.; Green, P. F. Control of the Entropic Interactions and Phase Behavior of Athermal Nanoparticle/Homopolymer Thin Film Mixtures. *Soft Matter* **2009**, *5*, 533−537.

(107) Tahir, M. N.; Eberhardt, M.; Theato, P.; Faiß, S.; Janshoff, A.; Gorelik, T.; Kolb, U.; Tremel, W. Reactive Polymers: A Versatile Toolbox for the Immobilization of Functional Molecules on TiO_2 Nanoparticles. *Angew. Chem., Int. Ed.* **2006**, *45*, 908−912.

(108) Fillery, S. P.; Koerner, H.; Drummy, L.; Dunkerley, E.; Durstock, M. F.; Schmidt, D. F.; Vaia, R. A. Nanolaminates: Increasing Dielectric Breakdown Strength of Composites. *ACS Appl. Mater. Interfaces* **2012**, *4*, 1388−1396.

(109) Tanaka, T.; Montanari, G.; Mulhaupt, R. Polymer Nanocomposites as Dielectrics and Electrical Insulation-Perspectives for Processing Technologies, Material Characterization and Future Applications. *IEEE Trans. Dielectr. Electr. Insul.* **2004**, *11*, 763−784.

(110) Thomas, P.; Dakshayini, B.; Mahadevaraju, G. High Permittivity Poly (Methyl Methacrylate)/Sr2timno6 Composites for High Energy Storage Capacitor Application. *Int. J. Curr. Eng. Technol.* **2013**, *Special Issue-1*, 129−134.

(111) Takala, M.; Ranta, H.; Nevalainen, P.; Pakonen, P.; Pelto, J.; Karttunen, M.; Virtanen, S.; Koivu, V.; Pettersson, M.; Sonerud, B. Dielectric Properties and Partial Discharge Endurance of Polypropylene-Silica Nanocomposite. *IEEE Trans. Dielectr. Electr. Insul.* **2010**, *17*, 1259−1267.

(112) Roy, M.; Nelson, J. K.; MacCrone, R. K.; Schadler, L. S. Candidate Mechanisms Controlling the Electrical Characteristics of Silica/Xlpe Nanodielectrics. *J. Mater. Sci.* **2007**, *42*, 3789−3799.

(113) Calebrese, C.; Hui, L.; Schadler, L. S.; Nelson, J. K. A Review on the Importance of Nanocomposite Processing to Enhance Electrical Insulation. *IEEE Trans. Dielectr. Electr. Insul.* **2011**, *18*, 938−945.

(114) Hong, J.; Winberg, P.; Schadler, L.; Siegel, R. Dielectric Properties of Zinc Oxide/Low Density Polyethylene Nanocomposites. *Mater. Lett.* **2005**, *59*, 473−476.

(115) Lewis, T. Interfaces and Nanodielectrics Are Synonymous. *IEEE Int. Conf. Solid Dielectr.* **2004**, *2*, 792−795.

(116) Nelson, J.; Reed, C.; Utracki, L.; MacCrone, R. Role of the Interface in Determining the Dielectric Properties of Nanocomposites. *IEEE Conf. Electr. Insul. Dielectr. Phenom.* **2004**, 314−317.

(117) Nelson, J. K. Overview of Nanodielectrics: Insulating Materials of the Future. *Electr. Insul. Conf. Electr. Manuf. Expo.* **2007**, 229−235.

(118) Roy, M.; Nelson, J.; MacCrone, R.; Schadler, L.; Reed, C.; Keefe, R. Polymer Nanocomposite Dielectrics-the Role of the Interface. *IEEE Trans. Dielectr. Electr. Insul.* **2005**, *12*, 629−643.

(119) Travelpiece, A.; Nelson, J.; Schadler, L.; Schweickart, D. Dielectric Integrity of High-Temperature Nanocomposites. *IEEE Conf. Electr. Insul. Dielectr. Phenom.* **2008**, 571−574.

(120) Zhang, C.; Stevens, G. C. The Dielectric Response of Polar and Non-Polar Nanodielectrics. *IEEE Trans. Dielectr. Electr. Insul.* **2008**, *15*, 606−617.

(121) Roy, M.; Nelson, J. K.; Schadler, L.; Zou, C.; Fothergill, J. C. The Influence of Physical and Chemical Linkage on the Properties of Nanocomposites. *IEEE Conf. Electr. Insul. Dielectr. Phenom.* **2005**, 183−186.

(122) Kuo, D.; Chang, C.; Su, T.; Wang, W.; Lin, B. Dielectric Properties of Three Ceramic/Epoxy Composites. *Mater. Chem. Phys.* **2004**, *85*, 201−206.

(123) Nelson, J.; Hu, Y.; Thiticharoenpong, J. Electrical Properties of TiO_2 Nanocomposites. *Annu. Rep. Conf. Electr. Insul. Dielectr. Phenom.* **2003**, 719−722.

(124) Nelson, J. K.; Fothergill, J. C. Internal Charge Behaviour of Nanocomposites. *Nanotechnology* **2004**, *15*, 586.

(125) Cao, Y.; Irwin, P. C.; Younsi, K. The Future of Nanodielectrics in the Electrical Power Industry. *IEEE Trans. Dielectr. Electr. Insul.* **2004**, *11*, 797−807.

(126) Calebrese, C.; Hui, L.; Schadler, L. S.; Nelson, J. K. Fundamentals for the Compounding of Nanocomposites to Enhance Electrical Insulation Performance. *IEEE Int. Power Modulator High Voltage Conf.* **2010**, 38−41.

(127) Ma, D.; Hugener, T. A.; Siegel, R. W.; Christerson, A.; Mårtensson, E.; Önneby, C.; Schadler, L. S. Influence of Nanoparticle Surface Modification on the Electrical Behaviour of Polyethylene Nanocomposites. *Nanotechnology* **2005**, *16*, 724−731.

(128) Dou, X.; Liu, X.; Zhang, Y.; Feng, H.; Chen, J.; Du, S. Improved Dielectric Strength of Barium Titanate-Polyvinylidene Fluoride Nanocomposite. *Appl. Phys. Lett.* **2009**, *95*, 132904.

(129) Kim, P.; Doss, N. M.; Tillotson, J. P.; Hotchkiss, P. J.; Pan, M. J.; Marder, S. R.; Li, J.; Calame, J. P.; Perry, J. W. High Energy Density Nanocomposites Based on Surface-Modified Batio3 and a Ferroelectric Polymer. *ACS nano* **2009**, *3*, 2581−2592.

(130) Akcora, P.; Liu, H.; Kumar, S. K.; Moll, J.; Li, Y.; Benicewicz, B. C.; Schadler, L. S.; Acehan, D.; Panagiotopoulos, A. Z.; Pryamitsyn, V. Anisotropic Self-Assembly of Spherical Polymer-Grafted Nanoparticles. *Nat. Mater.* **2009**, *8*, 354−359.

(131) Lai, M.; Yu, S.; Sun, R.; Zeng, X.; Luo, S.; Wong, C. P. Effects and Mechanism of Graft Modification on the Dielectric Performance of Polymer−Matrix Composites. *Compos. Sci. Technol.* **2013**, *89*, 127−133.

(132) Kanapitsas, A.; Pissis, P.; Kotsilkova, R. Dielectric Studies of Molecular Mobility and Phase Morphology in Polymer−Layered Silicate Nanocomposites. *J. Non-Cryst. Solids* **2002**, *305*, 204−211.

(133) Maity, P.; Poovamma, P.; Basu, S.; Parameswaran, V.; Gupta, N. Dielectric Spectroscopy of Epoxy Resin with and without Nanometric Alumina Fillers. *IEEE Trans. Dielectr. Electr. Insul.* **2009**, *16*, 1481−1488.

(134) Singha, S.; Thomas, M. J. Influence of Filler Loading on Dielectric Properties of Epoxy-Zno Nanocomposites. *IEEE Trans. Dielectr. Electr. Insul.* **2009**, *16*, 531−542.

(135) Artbauer, J. Electric Strength of Polymers. *J. Phys. D: Appl. Phys.* **1996**, *29*, 446.

(136) Schuman, T. P.; Siddabattuni, S.; Cox, O.; Dogan, F. Improved Dielectric Breakdown Strength of Covalently-Bonded Interface Polymer−Particle Nanocomposites. *Compos. Interfaces* **2010**, *17*, 719−731.

(137) Siddabattuni, S.; Schuman, T. P.; Dogan, F. Improved Polymer Nanocomposite Dielectric Breakdown Performance through Barium Titanate to Epoxy Interface Control. *Mater. Sci. Eng., B* **2011**, *176*, 1422−1429.

(138) Alig, I.; Jarek, M.; Hellmann, G. Restricted Segmental Mobility in Side-Chain Crystalline Comblike Polymers, Studied by Dielectric Relaxation Measurements. *Macromolecules* **1998**, *31*, 2245−2251.

(139) Bhimaraj, P.; Burris, D. L.; Action, J.; Sawyer, W. G.; Toney, C. G.; Siegel, R. W.; Schadler, L. S. Effect of Matrix Morphology on the Wear and Friction Behavior of Alumina Nanoparticle/Poly (Ethylene) Terephthalate Composites. *Wear* **2005**, *258*, 1437−1443.

(140) Yang, H.; Bhimaraj, P.; Yang, L.; Siegel, R. W.; Schadler, L. S. Crystal Growth in Alumina/Poly (Ethylene Terephthalate) Nanocomposite Films. *J. Polym. Sci., Part B: Polym. Phys.* **2007**, *45*, 747−757.

(141) Bhimaraj, P.; Yang, H.; Siegel, R. W.; Schadler, L. S. Crystal Nucleation and Growth in Poly (Ethylene Terephthalate)/Alumina-Nanoparticle Composites. *J. Appl. Polym. Sci.* **2007**, *106*, 4233−4240.

(142) Gao, L.; Tu, D.; Zhou, S.; Zhang, Z. The Influence of Morphology on the Electrical Breakdown Strength of Polypropylene Film. *IEEE Trans. Electr. Insul.* **1990**, *25*, 535−540.

(143) Tanaka, Y.; Ohnuma, N.; Katsunami, K.; Ohki, Y. Effects of Crystallinity and Electron Mean-Free-Path on Dielectric Strength of Low-Density Polyethylene. *IEEE Trans. Electr. Insul.* **1991**, *26*, 258−265.

(144) Li, J.; Seok, S. I.; Chu, B.; Dogan, F.; Zhang, Q.; Wang, Q. Nanocomposites of Ferroelectric Polymers with TiO_2 Nanoparticles Exhibiting Significantly Enhanced Electrical Energy Density. *Adv. Mater.* **2009**, *21*, 217−221.

(145) Umemori, M.; Taniike, T.; Terano, M. Influences of Polypropylene Grafted to SiO_2 Nanoparticles on the Crystallization Behavior and Mechanical Properties of Polypropylene/SiO_2 Nanocomposites. *Polym. Bull.* **2012**, *68*, 1093−1108.

(146) Ieda, M. Dielectric Breakdown Process of Polymers. *IEEE Trans. Electr. Insul.* **1980**, 206−224.

(147) Murugaraj, P.; Mainwaring, D.; Mora-Huertas, N. Dielectric Enhancement in Polymer-Nanoparticle Composites through Interphase Polarizability. *J. Appl. Phys.* **2005**, *98*, 054304.

(148) Todd, M. G.; Shi, F. G. Complex Permittivity of Composite Systems: A Comprehensive Interphase Approach. *IEEE Trans. Dielectr. Electr. Insul.* **2005**, *12*, 601−611.

(149) Virtanen, S.; Krentz, T. M.; Nelson, J. K.; Schadler, L. S.; Bell, M.; Benicewicz, B. C.; Hillborg, H.; Zhao, S. Dielectric Breakdown Strength of Epoxy Bimodal-Polymer-Brush-Grafted Core Functionalized Silica Nanocomposites. *IEEE Trans. Dielectr. Electr. Insul* **2014**, In press.

(150) Smith, R.; Liang, C.; Landry, M.; Nelson, J.; Schadler, L. The Mechanisms Leading to the Useful Electrical Properties of Polymer Nanodielectrics. *IEEE Trans. Dielectr. Electr. Insul.* **2008**, *15*, 187−196.

(151) Travelpiece, A.; Nelson, J.; Schadler, L.; Schweickart, D. Dielectric Integrity of Silica-Pai Nanocomposites at Elevated Temperature. *IEEE Conf. Electr. Insul. Dielectr. Phenom.* **2009**, 535−538.

(152) Siddabattuni, S.; Schuman, T. P.; Dogan, F. Dielectric Properties of Polymer−Particle Nanocomposites Influenced by Electronic Nature of Filler Surfaces. *ACS Appl. Mater. Interfaces* **2013**, *5*, 1917−1927.

(153) Zou, C.; Fothergill, J. C.; Rowe, S. W. The Effect of Water Absorption on the Dielectric Properties of Epoxy Nanocomposites. *IEEE Trans. Dielectr. Electr. Insul.* **2008**, *15*, 106−117.

(154) Ramdeen, T.; Dissado, L. A.; Hill, R. M. Influence of Adsorbed Water on the Dielectric Response of a Ceramic Material. *J. Chem. Soc., Faraday Trans. 1* **1984**, *80*, 325−340.

(155) Zhang, C.; Stevens, G. C. Dielectric Properties of Epoxy-Alumina Nanocomposites: The Effect of Absorbed Water. *IEEE Conf. Electr. Insul. Dielectr. Phenom.* **2006**, 325−328.

(156) Smith, R.; Hui, L.; Nelson, J.; Schadler, L. Interfacial Charge Behavior in Nanodielectrics. *IEEE Conf. Electr. Insul. Dielectr. Phenom.* **2009**, 650−653.

(157) Iyer, G.; Gorur, R.; Richert, R.; Krivda, A.; Schmidt, L. Dielectric Properties of Epoxy Based Nanocomposites for High Voltage Insulation. *IEEE Trans. Dielectr. Electr. Insul.* **2011**, *18*, 659−666.

(158) Chakraborty, H.; Sinha, A. Effect of Space Charge Density and High Voltage Breakdown of Surface Modified Alumina Reinforced Epoxy Composites. *Trans. Electr. Electron. Mater.* **2013**, *14*, 121−124.

(159) Sengupta, S. S.; Person, T. J.; Caronia, P. J. A New Generation of Tree-Retardant Crosslinked Polyethylene (TR-XLPE) Insulation. *Conf. Rec. IEEE Int. Symp. Electr. Insul.* **2010**, 1−6.

(160) Tao, P.; Li, Y.; Rungta, A.; Viswanath, A.; Gao, J.; Benicewicz, B. C.; Siegel, R. W.; Schadler, L. S. TiO_2 Nanocomposites with High Refractive Index and Transparency. *J. Mater. Chem.* **2011**, *21*, 18623−18629.

(161) Tao, P.; Viswanath, A.; Schadler, L. S.; Benicewicz, B. C.; Siegel, R. W. Preparation and Optical Properties of Indium Tin Oxide/Epoxy Nanocomposites with Polyglycidyl Methacrylate Grafted Nanoparticles. *ACS Appl. Mater. Interfaces* **2011**, *3*, 3638−3645.

(162) Ranjan, R.; Brittain, W. J. Combination of Living Radical Polymerization and Click Chemistry for Surface Modification. *Macromolecules* **2007**, *40*, 6217−6223.

(163) Ranjan, R.; Brittain, W. J. Synthesis of High Density Polymer Brushes on Nanoparticles by Combined RAFT Polymerization and Click Chemistry. *Macromol. Rapid Commun.* **2008**, *29*, 1104−1110.

(164) Ranjan, R.; Brittain, W. J. Tandem RAFT Polymerization and Click Chemistry: An Efficient Approach to Surface Modification. *Macromol. Rapid Commun.* **2007**, *28*, 2084−2089.

(165) Huang, Y.; Liu, Q.; Zhou, X.; Perrier, S. b.; Zhao, Y. Synthesis of Silica Particles Grafted with Well-Defined Living Polymeric Chains by Combination of RAFT Polymerization and Coupling Reaction. *Macromolecules* **2009**, *42*, 5509−5517.

(166) Pyun, J.; Jia, S.; Kowalewski, T.; Matyjaszewski, K. Synthesis and Surface Attachment of Abc Triblock Copolymers Containing Glassy and Rubbery Segments. *Macromol. Chem. Phys.* **2004**, *205*, 411−417.

(167) Li, Y.; Tao, P.; Viswanath, A.; Benicewicz, B. C.; Schadler, L. S. Bimodal Surface Ligand Engineering: The Key to Tunable Nanocomposites. *Langmuir* **2012**, *29*, 1211−1220.

(168) Hsiue, G. H.; Chu, L. W.; Lin, I. Optimized Phosphate Ester Structure for the Dispersion of Nano-Sized Barium Titanate in Proper Non-Aqueous Media. *Colloids Surf., A* **2007**, *294*, 212−220.

(169) Baum, M.; Brittain, W. J. Synthesis of Polymer Brushes on Silicate Substrates Via Reversible Addition Fragmentation Chain Transfer Technique. *Macromolecules* **2002**, *35*, 610−615.

(170) Cash, B. M.; Wang, L.; Benicewicz, B. C. The Preparation and Characterization of Carboxylic Acid-Coated Silica Nanoparticles. *J. Polym. Sci., Part A: Polym. Chem.* **2012**, *50*, 2533−2540.

(171) Huang, X.; Wirth, M. J. Surface-Initiated Radical Polymerization on Porous Silica. *Anal. Chem.* **1997**, *69*, 4577−4580.

(172) Husseman, M.; Malmström, E. E.; McNamara, M.; Mate, M.; Mecerreyes, D.; Benoit, D. G.; Hedrick, J. L.; Mansky, P.; Huang, E.; Russell, T. P. Controlled Synthesis of Polymer Brushes by "Living" Free Radical Polymerization Techniques. *Macromolecules* **1999**, *32*, 1424−1431.

(173) Li, C.; Benicewicz, B. C. Synthesis of Well-Defined Polymer Brushes Grafted onto Silica Nanoparticles Via Surface Reversible Addition-Fragmentation Chain Transfer Polymerization. *Macromolecules* **2005**, *38*, 5929−5936.

(174) Liu, C.; Pan, C. Grafting Polystyrene onto Silica Nanoparticles Via RAFT Polymerization. *Polymer* **2007**, *48*, 3679−3685.

(175) Lu, C.; Zhou, W.; Han, B.; Yang, H.; Chen, X.; Wang, X. Surface-Imprinted Core-Shell Nanoparticles for Sorbent Assays. *Anal. Chem.* **2007**, *79*, 5457−5461.

(176) Matyjaszewski, K.; Miller, P. J.; Shukla, N.; Immaraporn, B.; Gelman, A.; Luokala, B. B.; Siclovan, T. M.; Kickelbick, G.; Vallant, T.; Hoffmann, H. Polymers at Interfaces: Using Atom Transfer Radical Polymerization in the Controlled Growth of Homopolymers and Block Copolymers from Silicon Surfaces in the Absence of Untethered Sacrificial Initiator. *Macromolecules* **1999**, *32*, 8716−8724.

(177) Ohno, K.; Ma, Y.; Huang, Y.; Mori, C.; Yahata, Y.; Tsujii, Y.; Maschmeyer, T.; Moraes, J.; Perrier, S. Surface-Initiated Reversible Addition−Fragmentation Chain Transfer (RAFT) Polymerization from Fine Particles Functionalized with Trithiocarbonates. *Macromolecules* **2011**, *44*, 8944−8953.

(178) Pyun, J.; Jia, S.; Kowalewski, T.; Patterson, G. D.; Matyjaszewski, K. Synthesis and Characterization of Organic/Inorganic Hybrid Nanoparticles: Kinetics of Surface-Initiated Atom Transfer Radical Polymerization and Morphology of Hybrid Nanoparticle Ultrathin Films. *Macromolecules* **2003**, *36*, 5094−5104.

(179) Pyun, J.; Matyjaszewski, K.; Kowalewski, T.; Savin, D.; Patterson, G.; Kickelbick, G.; Huesing, N. Synthesis of Well-Defined Block Copolymers Tethered to Polysilsesquioxane Nanoparticles and Their Nanoscale Morphology on Surfaces. *J. Am. Chem. Soc.* **2001**, *123*, 9445−9446.

(180) Tsujii, Y.; Ejaz, M.; Sato, K.; Goto, A.; Fukuda, T. Mechanism and Kinetics of RAFT-Mediated Graft Polymerization of Styrene on a Solid Surface. 1. Experimental Evidence of Surface Radical Migration. *Macromolecules* **2001**, *34*, 8872−8878.

(181) Wang, L.; Benicewicz, B. C. Synthesis and Characterization of Dye-Labeled Poly (Methacrylic Acid) Grafted Silica Nanoparticles. *ACS Macro Lett.* **2013**, *2*, 173−176.

(182) Li, Y.; Schadler, L. S.; Benicewicz, B. C. In *Handbook of RAFT Polymerization*; Barner-Kowollik, C., Eds.; Wiley-VCH: Weinheim, Germany, 2008; Chapter 11, pp 423−453.

(183) Radhakrishnan, B.; Ranjan, R.; Brittain, W. J. Surface Initiated Polymerizations from Silica Nanoparticles. *Soft Matter* **2006**, *2*, 386−396.

(184) Pyun, J.; Matyjaszewski, K. Synthesis of Nanocomposite Organic/Inorganic Hybrid Materials Using Controlled/"Living" Radical Polymerization. *Chem. Mater.* **2001**, *13*, 3436−3448.

(185) Pyun, J.; Kowalewski, T.; Matyjaszewski, K. Synthesis of Polymer Brushes Using Atom Transfer Radical Polymerization. *Macromol. Rapid Commun.* **2003**, *24*, 1043−1059.

(186) Moraes, J.; Ohno, K.; Maschmeyer, T.; Perrier, S. Synthesis of Silica−Polymer Core−Shell Nanoparticles by Reversible Addition−Fragmentation Chain Transfer Polymerization. *Chem. Commun.* **2013**, *49*, 9077−9088.

(187) Minko, S.; Patil, S.; Datsyuk, V.; Simon, F.; Eichhorn, K. J.; Motornov, M.; Usov, D.; Tokarev, I.; Stamm, M. Synthesis of Adaptive Polymer Brushes Via "Grafting to" Approach from Melt. *Langmuir* **2002**, *18*, 289−296.

(188) Zhao, B.; He, T. Synthesis of Well-Defined Mixed Poly(Methyl Methacrylate)/Polystyrene Brushes from an Asymmetric Difunctional Initiator-Terminated Self-Assembled Monolayer. *Macromolecules* **2003**, *36*, 8599−8602.

(189) Huang, X.; Schmucker, A.; Dyke, J.; Hall, S. M.; Retrum, J.; Stein, B.; Remmes, N.; Baxter, D. V.; Dragnea, B.; Bronstein, L. M. Magnetic Nanoparticles with Functional Silanes: Evolution of Well-Defined Shells from Anhydride Containing Silane. *J. Mater. Chem.* **2009**, *19*, 4231−4239.

(190) White, M. A.; Johnson, J. A.; Koberstein, J. T.; Turro, N. J. Toward the Syntheses of Universal Ligands for Metal Oxide Surfaces: Controlling Surface Functionality through Click Chemistry. *J. Am. Chem. Soc.* **2006**, *128*, 11356−11357.

(191) Binder, W. H.; Weinstabl, H. C. Surface-Modified Superparamagnetic Iron-Oxide Nanoparticles. *Monatsh. Chem.* **2007**, *138*, 315−320.

(192) Lattuada, M.; Hatton, T. A. Functionalization of Monodisperse Magnetic Nanoparticles. *Langmuir* **2007**, *23*, 2158−2168.

(193) Peng, S.; Wang, C.; Xie, J.; Sun, S. Synthesis and Stabilization of Monodisperse Fe Nanoparticles. *J. Am. Chem. Soc.* **2006**, *128*, 10676−10677.

(194) Dong, A.; Ye, X.; Chen, J.; Kang, Y.; Gordon, T.; Kikkawa, J. M.; Murray, C. B. A Generalized Ligand-Exchange Strategy Enabling Sequential Surface Functionalization of Colloidal Nanocrystals. *J. Am. Chem. Soc.* **2010**, *133*, 998−1006.

(195) Hong, R.; Fischer, N. O.; Emrick, T.; Rotello, V. M. Surface PEGylation and Ligand Exchange Chemistry of FePt Nanoparticles for Biological Applications. *Chem. Mater.* **2005**, *17*, 4617−4621.

(196) Kim, M.; Chen, Y.; Liu, Y.; Peng, X. Super-Stable, High-Quality Fe_3O_4 Dendron−Nanocrystals Dispersible in Both Organic and Aqueous Solutions. *Adv. Mater.* **2005**, *17*, 1429−1432.

(197) Kim, S. B.; Cai, C.; Kim, J.; Sun, S.; Sweigart, D. A. Surface Modification of Fe_3O_4 and FePt Magnetic Nanoparticles with Organometallic Complexes. *Organometallics* **2009**, *28*, 5341−5348.

(198) Kovalenko, M. V.; Scheele, M.; Talapin, D. V. Colloidal Nanocrystals with Molecular Metal Chalcogenide Surface Ligands. *Science* **2009**, *324*, 1417−1420.

(199) Kovalenko, M. V.; Spokoyny, B.; Lee, J. S.; Scheele, M.; Weber, A.; Perera, S.; Landry, D.; Talapin, D. V. Semiconductor Nanocrystals Functionalized with Antimony Telluride Zintl Ions for Nanostructured Thermoelectrics. *J. Am. Chem. Soc.* **2010**, *132*, 6686−6695.

(200) Salgueiriño-Maceira, V.; Liz-Marzán, L. M.; Farle, M. Water-Based Ferrofluids from Fe_xPt_{1-x} Nanoparticles Synthesized in Organic Media. *Langmuir* **2004**, *20*, 6946−6950.

(201) Tangirala, R.; Baker, J. L.; Alivisatos, A. P.; Milliron, D. J. Modular Inorganic Nanocomposites by Conversion of Nanocrystal Superlattices. *Angew. Chem., Int. Ed.* **2010**, *49*, 2878−2882.

(202) Wei, Y.; Yang, J.; Ying, J. Y. Reversible Phase Transfer of Quantum Dots and Metal Nanoparticles. *Chem. Commun.* **2010**, *46*, 3179−3181.

(203) Xie, J.; Xu, C.; Kohler, N.; Hou, Y.; Sun, S. Controlled Pegylation of Monodisperse Fe_3O_4 Nanoparticles for Reduced Non-Specific Uptake by Macrophage Cells. *Adv. Mater.* **2007**, *19*, 3163−3166.

(204) Wu, N.; Fu, L.; Su, M.; Aslam, M.; Wong, K. C.; Dravid, V. P. Interaction of Fatty Acid Monolayers with Cobalt Nanoparticles. *Nano Lett.* **2004**, *4*, 383−386.

(205) Walther, A.; Müller, A. H. Janus Particles: Synthesis, Self-Assembly, Physical Properties, and Applications. *Chem. Rev.* **2013**, *113*, 5194−5261.

(206) Hu, J.; Zhou, S.; Sun, Y.; Fang, X.; Wu, L. Fabrication, Properties and Applications of Janus Particles. *Chem. Soc. Rev.* **2012**, *41*, 4356−4378.

(207) Wu, L. Y.; Ross, B. M.; Hong, S.; Lee, L. P. Bioinspired Nanocorals with Decoupled Cellular Targeting and Sensing Functionality. *Small* **2010**, *6*, 503−507.

(208) Hu, S. H.; Gao, X. Nanocomposites with Spatially Separated Functionalities for Combined Imaging and Magnetolytic Therapy. *J. Am. Chem. Soc.* **2010**, *132*, 7234−7237.

(209) Isojima, T.; Suh, S. K.; Vander Sande, J. B.; Hatton, T. A. Controlled Assembly of Nanoparticle Structures: Spherical and Toroidal Superlattices and Nanoparticle-Coated Polymeric Beads. *Langmuir* **2009**, *25*, 8292−8298.

(210) Qiang, W.; Wang, Y.; He, P.; Xu, H.; Gu, H.; Shi, D. Synthesis of Asymmetric Inorganic/Polymer Nanocomposite Particles Via Localized Substrate Surface Modification and Miniemulsion Polymerization. *Langmuir* **2008**, *24*, 606−608.

(211) Yin, Y.; Zhou, S.; You, B.; Wu, L. Facile Fabrication and Self-Assembly of Polystyrene−Silica Asymmetric Colloid Spheres. *J. Polym. Sci., Part A: Polym. Chem.* **2011**, *49*, 3272−3279.

(212) Xing, S.; Feng, Y.; Tay, Y. Y.; Chen, T.; Xu, J.; Pan, M.; He, J.; Hng, H. H.; Yan, Q.; Chen, H. Reducing the Symmetry of Bimetallic Au@ Ag Nanoparticles by Exploiting Eccentric Polymer Shells. *J. Am. Chem. Soc.* **2010**, *132*, 9537−9539.

(213) Verso, F. L.; Yelash, L.; Egorov, S. A.; Binder, K. Effect of the Solvent Quality on the Structural Rearrangement of Spherical Brushes: Coarse-Grained Models. *Soft Matter* **2012**, *8*, 4185−4196.

(214) Reith, D.; Milchev, A.; Virnau, P.; Binder, K. Computer Simulation Studies of Chain Dynamics in Polymer Brushes. *Macromolecules* **2012**, *45*, 4381−4393.

(215) Ndoro, T. V.; Voyiatzis, E.; Ghanbari, A.; Theodorou, D. N.; Böhm, M. C.; Müller-Plathe, F. Interface of Grafted and Ungrafted Silica Nanoparticles with a Polystyrene Matrix: Atomistic Molecular Dynamics Simulations. *Macromolecules* **2011**, *44*, 2316−2327.

(216) Ghanbari, A.; Ndoro, T. V.; Leroy, F. d. r.; Rahimi, M.; Böhm, M. C.; Müller-Plathe, F. Interphase Structure in Silica−Polystyrene Nanocomposites: A Coarse-Grained Molecular Dynamics Study. *Macromolecules* **2011**, *45*, 572−584.

(217) LoVerso, F.; Egorov, S. A.; Binder, K. Interaction between Polymer Brush-Coated Spherical Nanoparticles: Effect of Solvent Quality. *Macromolecules* **2012**, *45*, 8892−8902.

(218) Ndoro, T. V.; Böhm, M. C.; Müller-Plathe, F. Interface and Interphase Dynamics of Polystyrene Chains near Grafted and Ungrafted Silica Nanoparticles. *Macromolecules* **2011**, *45*, 171−179.

(219) Milchev, A.; Binder, K. Semiflexible Polymers Grafted to a Solid Planar Substrate: Changing the Structure from Polymer Brush to "Polymer Bristle. *J. Chem. Phys.* **2012**, *136*, 194901.

(220) Egorov, S.; Binder, K. Effect of Solvent Quality on the Dispersibility of Polymer-Grafted Spherical Nanoparticles in Polymer Solutions. *J. Chem. Phys.* **2012**, *137*, 094901.

(221) Vlassopoulos, D. Colloidal Star Polymers: Models for Studying Dynamically Arrested States in Soft Matter. *J. Polym. Sci., Part B: Polym. Phys.* **2004**, *42*, 2931−2941.

(222) Chevigny, C.; Jestin, J.; Gigmes, D.; Schweins, R.; Di-Cola, E.; Dalmas, F.; Bertin, D.; Boué, F. Wet-to-Dry" Conformational Transition of Polymer Layers Grafted to Nanoparticles in Nanocomposite. *Macromolecules* **2010**, *43*, 4833−4837.

(223) Kumar, S. K.; Jouault, N.; Benicewicz, B.; Neely, T. Nanocomposites with Polymer Grafted Nanoparticles. *Macromolecules* **2013**, *46*, 3199−3214.

(224) Koo, J. H. *Polymer Nanocomposites: Processing, Characterization, and Applications*; McGraw-Hill: New York, 2006.

(225) Mittal, V. In *Characterization Techniques for Polymer Nanocomposites*; Mittal, V., Ed.; Wiley-VCH: Weinheim, Germany, 2012; Chapter 1, pp 1−12.